(19) Europäisches Patentamt
European Patent Office
Office européen des brevets

(11) **EP 1 957 686 B1**

(12) **EUROPEAN PATENT SPECIFICATION**

(45) Date of publication and mention of the grant of the patent:
04.08.2010 Bulletin 2010/31

(21) Application number: **06775159.4**

(22) Date of filing: **29.08.2006**

(51) Int Cl.:
C22C 45/10 *(2006.01)* ***C22C 32/00*** *(2006.01)*
C22C 16/00 *(2006.01)*

(86) International application number:
PCT/CH2006/000466

(87) International publication number:
WO 2007/038882 (12.04.2007 Gazette 2007/15)

(54) BULK METALLIC GLASS/GRAPHITE COMPOSITES

VERBUNDWERKSTOFFE AUS METALLISCHEM MASSIVGLAS UND GRAPHIT

COMPOSITES DE GRAPHITE/VERRE MÉTALLIQUE MASSIF

(84) Designated Contracting States:
AT BE BG CH CY CZ DE DK EE ES FI FR GB GR HU IE IS IT LI LT LU LV MC NL PL PT RO SE SI SK TR

(30) Priority: **03.10.2005 US 722409 P**

(43) Date of publication of application:
20.08.2008 Bulletin 2008/34

(73) Proprietor: **ETH Zurich**
8092 Zurich (CH)

(72) Inventors:
- **LÖFFLER, Jörg, F.**
  CH-5425 Schneisingen (CH)
- **SIEGRIST, Marco**
  CH-8906 Bonstetten (CH)

(74) Representative: **Detken, Andreas et al**
Isler & Pedrazzini AG
Gotthardstrasse 53
Postfach 1772
8027 Zürich (CH)

(56) References cited:
- **HIRANO, TOMOYA ET AL: "Synthesis and mechanical properties of Zr55Al10Ni5Cu30 bulk glass composites containing ZrC particles formed by the in-situ reaction" MATERIALS TRANSACTIONS, JIM , 41(11), 1454-1459 CODEN: MTJIEY; ISSN: 0916-1821, 2000, XP001247781**
- **SZUECS, F. ET AL: "Preparation , microstructure and mechanical properties of carbon fiber containing bulk metallic glass composites" MATERIALS SCIENCE FORUM , 360-362 (METASTABLE, MECHANICALLY ALLOYED AND NANOCRYSTALLINE MATERIALS), 43-48 CODEN: MSFOEP; ISSN: 0255-5476, 2001, XP001248001**
- **KATO, HIDEMI ET AL: "Synthesis and viscoelasticity of Zr-based bulk glassy alloy containing ZrC particles" MATERIALS RESEARCH SOCIETY SYMPOSIUM PROCEEDINGS , 644(SUPERCOOLED LIQUID, BULK GLASSY AND NANOCRYSTALLINE STATES OF ALLOYS), L11.9/1-L11.9/6 CODEN: MRSPDH; ISSN: 0272-9172, 2001, XP001247789**
- **CHEN, FENG ET AL: "Crystallization of Zr55Al10Ni5Cu30 bulk metallic glass composites containing ZrC particles" MATERIALS TRANSACTIONS , 43(1), 1-4 CODEN: MTARCE; ISSN: 1345-9678, 2002, XP001247780**
- **KATO, HIDEMI ET AL: "Synthesis and mechanical properties of bulk amorphous Zr-Al-Ni-Cu alloys containing ZrC particles" MATERIALS TRANSACTIONS, JIM , 38(9), 793-800 CODEN: MTJIEY; ISSN: 0916-1821, 1997, XP001247779**

Note: Within nine months of the publication of the mention of the grant of the European patent in the European Patent Bulletin, any person may give notice to the European Patent Office of opposition to that patent, in accordance with the Implementing Regulations. Notice of opposition shall not be deemed to have been filed until the opposition fee has been paid. (Art. 99(1) European Patent Convention).

EP 1 957 686 B1

Description

Field of the invention

[0001] The present invention relates to a composite material having a first, amorphous alloy phase forming a substantially continuous matrix and having a second, reinforcing phase embedded in the matrix.

Background of the invention

[0002] Many amorphous metallic alloys with good glass-forming ability have been developed over the last few years. These bulk metallic glasses (BMGs) possess very interesting mechanical, magnetic, thermophysical and structural properties. They display, for example, up to double the fracture strength and four times the elasticity of their crystalline counterparts and thus have a very high potential for use as structural materials. Unfortunately, these properties cannot be fully exploited due to the alloys' brittle fracture behavior. With no crystalline structure, deformation via dislocation movement is impossible, but takes place in one or a few highly-localized shear bands. Even though BMGs may show some type of "ductile" fracture mechanism on a microscopic scale, metallic glasses are generally brittle because the fracture energy is concentrated in a very small volume of the sample. Drastic enhancement of the plasticity of BMGs would lead to a revolutionary new material for structural applications.

[0003] Achieving this increase in plasticity is a very timely topic, and many researchers are working on it using different approaches. Foreign-particle-reinforced BMGs, *in-situ*-formed BMG composites, porous Pd-based BMGs, and monolithic Pt-based BMGs displaying a high Poisson ratio have been investigated. All approaches have one thing in common, namely the intention to increase shear-band density so that fracture energy will be distributed over a larger volume of the sample.

[0004] Foreign-particle reinforcement appears to be particularly promising. The materials so far employed as foreign particles for reinforcement include ductile metals like W, Ta, Nb, Mo or steel and ceramics like WC, TiC, SiC or ZrC.

[0005] However, it is believed that the properties, in particular, plasticity in relation to yield strength, of such previously disclosed foreign-particle-reinforced BMGs are not yet at their optimum.

[0006] Reinforcement by structures other than particles, such as sheets, fibers or wires, has also been suggested. In particular, reinforcement by carbon fibers or carbon nanotubes has been disclosed in:

- Kim, C. P., Busch, R., Masuhr, A., Choi-Yim, H. & Johnson, W. L. "Processing of Carbon-Fiber-Reinforced Zr41.2Ti13.8Cu12.5Ni10.0Be22.5 Bulk Metallic Glass Composites". Appl. Phys. Lett. 79, 1456-1458 (2001).
- Bian, Z. et al., "Carbon-nanotube-reinforced Zr52.5Cu17.9Ni14.6Al10Ti5 bulk metallic glass composites", Appl. Phys. Lett. 81, 4739-4741 (2002);
- Bian, Z. et al., "Carbon-nanotube-reinforced Zr-based bulk metallic glass composites and their properties", Adv. Funct. Mater. 14, 55-63 (2004).

[0007] However, BMGs reinforced by carbon fibers will have anisotropic properties, while alloys reinforced by carbon nanotubes have a strong tendency to crystallize because the small nanotubes act as heterogeneous nucleation sites. They have been shown to be even more brittle than the corresponding monolithic BMG. In addition, carbon nanotubes are relatively expensive to produce.

[0008] *In-situ* formed BMG composites have been shown to display good combinations of yield strength and plasticity. In particular, examples for zirconium carbide (ZrC) reinforcement are disclosed in the following publications:

- Wang, W. H. & Bai, H. Y. "Carbon-addition-induced bulk ZrTiCuNiBe amorphous matrix composite containing ZrC particles". Mater. Lett. 44, 59-63 (2000).
- Kato, H., Hirano, T., Matsuo, A., Kawamura, Y. & Inoue, A. "High strength and good ductility of Zr55Al10Ni5Cu30 bulk glass containing ZrC particles". Scr. Mater. 43, 503-507 (2000).
- Hirano, T., Kato, H., Matsuo, A., Akihisa & Inoue, A. "Synthesis and mechanical properties of Zr55Al10Ni5Cu30 bulk glass composites containing ZrC particles formed by the in-situ reaction". Mater. Trans. JIM 41, 1454-1459 (2000).
- Chen, F. et al. "Crystallization of Zr55Al10Ni5Cu30 Bulk Metallic Glass Composites Containing ZrC Particles". Mater. Trans. JIM 43, 1-4 (2002).
- Szuecs et al., 'Preparation, microstructure and mechanical properties of carbon fiber containing bulk metallic glass composites', Materials Science Forum, (2001), vol 360-362, pp. 43-48.

Summary of the invention

[0009] It is an object of the present invention to provide a composite material with an amorphous alloy phase that has a high plasticity, in particular, a material having a high plasticity while at the same time having a high yield strength.

[0010] It is a further object of the present invention to provide a composite material with an amorphous alloy phase that has improved thermal stability.

[0011] It is a further object of the present invention to provide a composite material with an amorphous alloy phase that has improved tribological properties, in particular, a low coefficient of friction and a good resistance to abrasion.

[0012] These and other objects are achieved by a composite material according to claim 1, the method of claim 20 relating to its manufacture.

[0013] Thus, there is provided a composite material having at least two phases. The composite material comprises

- a substantially amorphous first phase forming a substantially continuous matrix, the first phase consisting essentially of a (metallic) alloy; and
- a second phase embedded in said matrix, said second phase comprising graphite particles.

[0014] By embedding graphite particles in the amorphous alloy matrix (BMG matrix), a remarkable increase in plasticity is achieved, while yield strength and elasticity remain comparable to that of the monolithic amorphous alloy. At the same time, favorable properties under friction, such as a low coefficient of friction (COF) and high resistance to abrasion are obtained, which makes the composite material according to the present invention a good candidate for dry sliding applications, such as frictional (plain) bearings. Furthermore, the thermal stability is increased as compared to the monolithic matrix material, i.e., the onset of crystallization is shifted to higher temperatures.

[0015] In the context of the present invention, the term "graphite" is to be understood to designate a form of elemental carbon in which substantially all carbon atoms (or at least their vast majority) exist in a sp2-hybridized state. In a perfect graphite structure, the carbon atoms are arranged in layers having a hexagonal structure. However, in more general terms, the term "graphite" is to be understood to also include structurally less well-defined materials such as pyrolytic carbon, in which the layers are to some extent covalently bonded, or soot, in particular carbon black, which may consist essentially of carbon in a predominantly amorphous state.

[0016] The term "particle" is to be understood to designate a small body having no well-defined axis of symmetry or approximate symmetry and having roughly similar dimensions along all directions in space. In particular, the term "particle" is to be understood as excluding fibers, which extend along a preferred direction, or (nano-) tubes, which likewise have a preferred direction (approximate axis of symmetry). Fibers or nanotubes, when used as a reinforcing material, impart very different properties to a material than particles do.

[0017] The particles used in the present invention may have a broad size range. There is lower limit to the size of 1 micrometer; however, for some matrix alloys, it has been found difficult to prevent graphite particles smaller than about 10 micrometers from completely reacting with the matrix alloy to form carbides. Therefore, a minimum dimension of about 10 micrometers, preferably about 25 micrometers is preferred. There is also no "hard" upper limit for the size of the graphite particles. However, in practical terms, often the size will be less than about 200 micrometers. Preferably, the graphite particles have a size in the range between about 25 and about 75 micrometers. The term "size" is to be understood as designating an average of the dimensions of the particles over all directions in space.

[0018] A very broad range for the volume fraction of the second (reinforcing) phase relative to the total volume of the composite material is possible. Significant effects are expected if the second phase locally occupies at least 3 volume percent of the total volume of the composite material. On the other hand, the theoretical maximum volume fraction of the second phase is only limited by the situation in which the particles are so densely distributed that all the particles would touch each other. This volume fraction is between 1 volume percent and 20 volume percent. The most preferred range depends on the average particle size. For larger particles, a lower volume fraction appears to be advantageous. By the way of example, for particles with sizes in the range between about 25 and about 45 micrometers, a volume fraction of the second phase in the range between 3 and about 10 volume percent is preferred, leading to a marked increase in plasticity and a marked decrease in COF, while yield strength and hardness are only moderately affected. For particles with sizes in the range from about 45 to about 75 micrometers, the preferred volume ratio is between 3 and about 6 volume percent. Of course, the exact amount will also depend on the desired application. It will also depend on the processing conditions, as will become more clear below, when the formation of carbide layers is discussed.

[0019] The volume fraction or concentration of the second phase may vary over the volume of an object made from the material, e.g., the concentration of the second phase may be higher near the surface of an object than in the bulk. This is especially advantageous if the object is to be used in a dry bearing application, where mainly the surface properties are of interest.

[0020] An important effect of the graphite particles is to induce the formation of closely spaced shear bands throughout the material if a sample of the material is deformed. After compressive deformation of the composite material up to yield, the density of shear bands can easily be determined from optical images of the fracture surface. Preferably, the properties of the second phase (shape and size distribution of the graphite particles, volume fraction etc.) are chosen such that shear bands are spaced apart by less than about 5 micrometers around the graphite particles. Preferably, the shear bands are preferably substantially uniformly (homogeneously) distributed over regions substantially larger than an average graphite particle, preferably over the whole matrix.

[0021] In order to ensure good mixing and close contact (on the atomic scale) of the phases and a uniform distribution of the second phase in the matrix, the matrix alloy, in the liquid state, is preferably capable of wetting the particles of the second phase. In other words, the surface of the particles is preferably wettable by the (liq-

uid) matrix alloy. Wettability is usually quantified by the so-called contact angle. A surface is normally considered to be wettable by a liquid if the contact angle is below 90°. Liquid metals which are known to be capable of wetting graphite surfaces include, in particular, zirconium, titanium, copper and iron. Alloys containing a major proportion (e.g., at least about 40%) of one or more of these metals are expected to have a good wetting behavior.

[0022] Another quantity which is relevant in the formation of the composite materials according to the present invention is the reactivity between the alloy and graphite to form carbides. Such a reaction on the particle surface is, to some extent, desired as it ensures a very close atomic bonding between the two phases, and as it can be used to tailor the properties of the composite material. This will be discussed in more detail below. A reaction between the alloy and the graphite particles will take place if the enthalpy of formation of metal carbides is negative. Therefore, it is preferred that the alloy comprises at least about 40 atomic percent of one or more metals having a negative enthalpy of formation for the reaction with graphite to form a metal carbide. Examples include zirconium and titanium.

[0023] Preferably, the alloy is a Zr-based alloy, i.e., it comprises at least about 40 atomic percent of zirconium. Zirconium is known to have a negative enthalpy of formation with graphite to form ZrC (-106 kJ/mol) and to have a good wetting behavior for graphite. Due to the well-known reaction behavior between Zr and graphite, it may reasonably be expected that all Zr-based BMGs are suitable matrix alloys for the composite materials of the present invention. Many Zr-based alloys with good glass-forming abilities (Zr-based BMGs) have been developed to date with widely varying compositions. A non-exhaustive list of examples includes:

- $Zr_{58}Cu_{22}Fe_8Al_{12}$ (Bio 1);
- $Zr_{57}Nb_5Al_{10}Cu_{15.4}Ni_{12.6}$ (Vit 106);
- $Zr_{41.2}Ti_{13.8}Cu_{12.5}Ni_{10}Be_{22.5}$ (Vit 1);
- $Zr_{46.75}Ti_{8.8}Ni_{10}Cu_{7.5}Be_{27.5}$(Vit 4);
- $Zr_{60}Al_{10}Cu_{30}$, $Zr_{55}Al_{15}N1_{25}$, $Zr_{55}Cu_{30}Al_{10}Ni_5$, $Zr_{55}Ti_5Al_{10}Cu_{20}Nl_{10}$, and $Zr_{52.5}Ti_5Al_{12.5}Cu_{20}Ni_{10}$;
- Alloy of composition $(Zr_xCu_{100-x})_{80}(Fe_{40}Al_{60})_{20}$ with . Such alloys have been investigated extensively in WO 2006/026882, whose contents are incorporated herein by reference for teaching bulk metallic glasses following specific principles in their atomic composition. In particular, alloys with x = 62, 64, 66, 68, 72.5, 77, 79, 81 or 83 have been investigated.
- Further examples from WO 2006/026882 include:

  $(Zr_{95}Ti_5)_{72}Cu_{13}Fe_{13}Al_2$, $Zr_{70}Cu_{13}Fe_{13}Al_3Sn_1$, $Zr_{70}Cu_{13}Fe_{13}Al_2Cr_2$, $Zr_{70}Cu_{13}Fe_{13}Al_2Nb_2$, $Zr_{70}Cu_{13}Fe_{13}Al_2Zn_2$, $(Zr_{72}Cu_{13}Fe_{13}Al_2)_{98}MO_2$,

  $(Zr_{72}Cu_{13}Fe_{13}Al_2)_{98}P_2$, $(Z_{95}Hf_5)_{72}Cu_{13}Fe_{13}Al_2$, $Zr_{70}Cu_{11}Fe_{11}Al_8$, $Zr_{71}Cu_{11}Fe_{10}Al_8$, $(Zr_{74}Cu_{13}Fe_{13})_{90}Al_{10}$, $Zr_{72}Cu_{13}Fe_{13}Al_2$, $(Zr_{74}Cu_{13}Fe_{13})_{98}Al_2$, $Zr_{73}Cu_{13}Fe_{31}4l_1$, $Zr_{72}Cu_{13}Fe_{13}Al_2$, $Zr_{71}Cu_{13}Fe_{13}Al_3$, $Zr_{72}Cu_{12}Fe_{12}Al_4$, $Zr_{70}Cu_{13}Fe_{13}Al_4$, $Zr_{72}Cu_{11}Fe_{11}Al_6$, $Zr_{72}Cu_{11.5}Fe_{11}Al_{5.5}$, $Zr_{73}Cu_{11}Fe_{11}Al_5$, $Zr_{71}Cu_{11}Fe_{11}Al_7$, $Zr_{69}Cu_{11}Fe_{11}Al_9$, $Zr_{70}Cu_{10.5}Fe_{10.5}Al_9$, $Zr_{70}Cu_{10}Fe_{11}Al_9$, $Zr_{70}Cu_{11}Fe_{10}Al_9$, $Zr_{69}Cu_{10}Fe_{10}Al_{11}$, $Zr_{69}Cu_{10}Fe_{11}Al_{10}$, $Zr_{70}Cu_{13}Fe_{13}Al_2Sn_2$, $Zr_{72}Cu_{13}Fe_{13}Sn_2$, $(Zr_{74}Cu_{13}Fe_{13})_{98}Sn_2$, $(Zr_{79}Cu_{21})_{80}(Fe_{40}Al_{60})_{20}$, $(Zr_{81}Cu_{19})_{80}(Fe_{40}Al_{60})_{20}$, $(Zr_{83}Cu_{17})_{80}(Fe_{40}Al_{60})_{20}$, $(Zr_{66}Cu_{34})_{80}(Fe_{40}Al_{60})_{20}$, $(Zr_{64}Cu_{36})_{80}(Fe_{40}Al_{60})_{20}$, and $(Zr_{62}Cu_{38})_{80}(Fe_{40}Al_{60})_{20}$.

[0024] Extensive experiments, to be described in more detail below, have in particular been performed for composites whose matrix alloy is represented essentially by the chemical formula $Zr_{52.5}Cu_{17.9}Ni_{14.6}Al_{10}Ti_5$. This alloy has excellent glass-forming ability and has become known as "Vit 105". For a Vit 105 matrix reinforced by graphite particles in the size range of about 25 micrometers to about 45 micrometers, a plasticity of up to 15% under compression and a yield strength of up to 1.5 GPa has been achieved. For reinforcement with particles in the size range of about 45 micrometers to about 75 micrometers, a plasticity of up to 18.5% under compression and a yield strength of up to 1.85 GPa has been achieved.

[0025] The mechanical properties of the composite material can be tailored by providing graphite particles having a core of graphite covered at least partially by a interfacial carbide layer. In other words, in a preferred embodiment, at least a fraction of the graphite particles have a core consisting essentially of graphite and an interfacial layer comprising at least one metal carbide, in particular, an interfacial layer consisting essentially of zirconium carbide. The layer is preferably formed *in situ* by a reaction of graphite with at least one metal in the surrounding matrix (interfacial carbide formation *in situ*).

[0026] The interfacial layer may be very thin and might amount to only a few atomic layers. For many alloys, such a layer might even be unavoidable due to unavoidable *in-situ* reactions during processing. A thin interfacial layer, formed *in situ*, will ensure an intimate contact between particle and matrix, without much influence on other properties. A thicker layer will also alter the mechanical properties of the composite material, such as plasticity, yield strength and, in particular, hardness, which increases with increasing thickness of the layer. For applications where an increased hardness is desired, it is advantageous if the interfacial layer has a thickness of at least 100 nanometers. On the other hand, it is advantageous if the thickness does not exceed about 1.5 to 2 micrometers and is preferably below about 1 micrometer, in order

not to induce a too brittle fracture behavior.

[0027] In order to avoid that the graphite particles fully transform into carbide particles, it is advantageous if they are not too small. In particular, it is advantageous if the graphite particles, including the interfacial carbide layer, have a size of at least about 25 micrometers. This is especially true for Zr-based matrix alloys.

[0028] The present invention further provides a three-phase composite material that, in addition to the alloy matrix phase and the graphite particle phase, comprises a third phase embedded in the matrix, wherein the third phase comprises particles.

[0029] The third phase may comprise crystalline particles that are composed of the same elements as the matrix alloy. Such particles are usually formed during the cooling of the matrix alloy from the melt. In particular, these particles may be nanocrystals with a mean size below about 1 micrometer. To some extent, their presence might be unavoidable; however, the processing conditions may also be deliberately chosen such that a considerable fraction of such particles is formed, e.g., up to 30 or 50%. These particles will normally be composed of the same elements as the matrix alloy, however, with different atomic fractions of the individual elements.

[0030] Alternatively or additionally, the third phase may comprise carbide particles. While the carbide particles may be preformed and added to the matrix, preferably the carbide particles are formed *in situ* by a reaction of graphite with the alloy. Such particles may be formed by different mechanisms. In one example, they may result from a substantially complete transformation of relatively small graphite particles with at least one metal component of the alloy into the corresponding carbide, with at most traces of graphite remaining. In another example, they are the result of a mechanism in which metal carbide that has formed on the surface of (larger) graphite particles has been separated from this surface, e.g., by strong stirring, and dispersed in the matrix. In a preferred embodiment, the carbide particles consist essentially of zirconium carbide.

[0031] The carbide particles preferably have a size of less than or equal to about 10 micrometers. In particular, such particles can readily be formed *in situ* by a complete transformation of similarly small graphite particles by a reaction with the matrix alloy.

[0032] The various composite materials according the present invention may be used in a variety of different applications in which one or more of the following properties are required: high plasticity, high yield strength, high elasticity, high elastic constants, low coefficient of friction, high resistance to abrasion. One example are articles employed in a dry frictional (plain) bearing. In particular, the two-phase composite materials described above, with graphite particles having no or only a minimal interfacial carbide layer, are promising for such applications. If higher hardness is additionally required, the three-phase composite materials described above, with both graphite parties and carbide particles, are advantageous. Another example where, in addition to low COF, high plasticity and high yield strength are important, are joints, in particular small joints which experience comparably high loads such as joints between different parts of a mobile telephone. Also for such applications the materials of the present invention are particularly advantageous. A further field of application are springs. Metallic glasses are known to display an elastic limit which is 2-4 times larger than for their crystalline counterparts. However, for technological applications the large elastic limit cannot be fully exploited due to the brittle fracture behavior of the monolithic material. The plasticity achieved with the composites in this invention allow a spring design fully exploiting the potential of the matrix material.

[0033] The composite material of the present invention may be prepared by various methods. In an advantageous process an alloy with good glass-forming capabilities is provided. A good glass former is capable of retaining an amorphous state when cooled from its melt at or above a critical cooling rate, where the critical cooling rate is no more than about 1000 K per second, preferably no more than about 100 K per second. The process then comprises the following steps:

- heating the alloy above its liquidus temperature to form a liquid alloy;
- dispersing graphite powder in the liquid alloy to form a finely dispersed mixture;
- cooling the mixture below its glass transition temperature sufficiently rapidly for forming a composite material comprising an amorphous, substantially continuous alloy matrix with a second phase embedded in said matrix, said second phase comprising graphite particles.

[0034] In such a process, the alloy may be heated above its liquidus temperature by induction melting on top of the graphite powder. Before the final cooling step, the alloy may optionally be processed once or repeatedly at a temperature above the melting (liquidus) temperature for a time sufficiently long for a carbide layer to form on the surface of said graphite particles. If a three-phase alloy is desired, the mixture may be processed once or repeatedly at a temperature above said melting temperature for a time sufficiently long for a fraction of said graphite particles reacting with at least one metal component of said alloy to form metal carbide particles. In this case, it is advantageous if the graphite powder initially dispersed into the alloy has a bimodal size distribution of the graphite particles, with a fraction of particles smaller than about 25 micrometers, preferably smaller than about 10 micrometers, and another fraction of particles larger than about 25 micrometers.

Brief description of the drawings

[0035] The invention will be described in more detail in connection with exemplary embodiments illustrated in

the drawings, in which

Fig. 1 shows an optical microscopy image of a graphite-particle- reinforced BMG composite with 5 vol. % graphite;

Fig. 2 shows differential scanning calorimetry (DSC) scans of monolithic Vit 105 and BMG-graphite composites with varying graphite parti- cle volume content;

Fig. 3 shows x-ray diffraction (XRD) scans of BMG-graphite composites with 3.5 vol.% graphite reinforcement produced at different casting temperature;

Fig. 4 shows compressive stress-strain curves and hardness (inset) for as-cast 3 mm graphite-reinforced Vit 105 composites of various re- inforcement contents;

Fig. 5 shows compressive stress-strain curves for as-cast 3 mm graph- itereinforced Vit 105 composites with optimized size and process parameters;

Fig. 6 shows a comparison of strength and plasticity derived from Figs. 4 and 5 to literature values;

Fig. 7A-7E shows scanning electron microscopy (SEM) images of fracture surfaces and particle-shear band interactions;

Fig. 8 shows XRD scans for three samples designated as sample 1 to 3, having 5 vol.% graphite reinforcement and increasing interfacial carbide content;

Fig. 9 shows stress-strain curves for samples 1 to 3;

Fig. 10A and 10B show optical microscopy images of samples 1 and 3, respec- tively, illustrating different extents of carbide formation along the matrix-particle interface;

Fig. 11 shows a diagram illustrating the hardness of composites processed at 0.35 kW and 2.1 kW power input compared to the mono- lithic matrix material;

Fig. 12 shows an optical micrograph of a graphite/ZrC reinforced BMG;

Fig. 13 shows XRD scans of three kinds of composites described above;

Fig. 14 show a schematic setup for measuring tribological properties;

Fig. 15 shows an SEM image showing an overview of wear tracks made at different parameters on a composite sample containing 8 vol.% graphite;

Fig. 16 shows XRD scans of a composite with 4 vol.% graphite and 3 vol.% graphite with *in situ* formed ZrC before and after tribology testing;

Fig. 17 shows a diagram illustrating the COF in dependence of graphite content for composites with and without *in situ* ZrC formation. For the composites with *in situ* ZrC formation the COF in the upper and lower regime is shown.

Detailed description of the invention

[0036] For achieving the goal of obtaining improved BMG-based materials, it is believed that foreign-particle reinforcement has the brightest future, because it allows easy reproducibility and direct tailoring of material properties. Foreign-particle-reinforced BMGs display, for example, better reproducibility of microstructure than *in-situ*-formed composites because the reinforcement microstructure and volume content are independent of processing parameters, in particular cooling rate. Similarly, while porous BMGs display a combination of high plasticity and yield strength, achieving a homogeneous pore distribution is very difficult. Monolithic BMGs with high poisson ratios also appear promising, but the effect of enhanced plasticity has only been observed so far in a very costly Pt-based alloy. Foreign-particle reinforcement also has the great advantage that the microstructure and thus the material properties can be tailored. The latter can be adjusted by type, shape, size and volume fraction of the reinforcement particles, as it is state-of-the-art in crystalline metal-matrix composites (MMCs) Foreign-particle reinforced BMGs also display high reproducibility because they can be processed by standard MMC processing techniques followed by a rapid quenching step. By using reinforcement particles in the micrometer range, the heterogeneous nucleation surface can be minimized, so that a high critical casting thickness is still achieved with today's good glass-formers.

[0037] In the following, a new class of foreign-particle-reinforced BMGs is discussed, where a fully amorphous alloy matrix was reinforced with graphite particles. In the following examples, $Zr_{52.5}Cu_{17.9}Al_{10}Ni_{14.6}Ti_5$ (Vit 105) was employed. The reinforcing particles had sizes of 25-44 μm and, in some cases, 44-75 μm. Of course, the invention is in no way limited to this base BMG or these particle sizes. A plasticity of up to 18.5% was achieved without sacrificing the high yield strength (1.85 GPa) of the metallic glass. Its microstructure can be reproduced easily and is independent of cooling rate. This novel composite displays the highest combination of yield strength and ductility reported so far for foreign-particle-reinforced BMGs, and the mechanical properties remain favorable,

even if compared to amorphous alloys or composites produced by the other methods discussed above.

Characterization of graphite-reinforced BMGs

[0038] Figure 1 shows, as an example, the graphite particle distribution in the Vit 105 matrix for a composite containing 5 vol.% graphite at 25-44 μm particle size, as obtained by induction mixing. The particles are homogeneously distributed in the glassy Vit 105 matrix and have shapes ranging from rectangular to circular.

[0039] Figure 2 shows DSC scans of monolithic Vit 105 and of the composites with various reinforcement volume fractions ranging from 5 to 20 vol.% at 25-44 μm particle size. A comparison of the crystallization enthalpy of the composites with that of monolithic Vit 105 shows that the matrix material is fully amorphous. The addition of graphite, however, shifts the onset of crystallization to a higher temperature, i.e. the composite has a higher thermal stability than the monolithic metallic glass, and the crystallization behavior changes. The first crystallization peak increases with increasing graphite content at the expense of the second crystallization event.

[0040] Figure 3 shows XRD scans for a Vit 105 composite with 3.5 vol.% graphite at 25-44 μm particle size at different casting temperatures. The two clearly seen amorphous humps result from the glassy Vit 105 matrix, while the Bragg peaks can be attributed to crystalline ZrC. While only traces of ZrC are observed in the lower scan, the ZrC content increases significantly with increasing casting temperature. The graphite peaks are not visible in the XRD scans because carbon is too light to be detected compared to the other elements present. It was found by energy-dispersive x-ray diffraction (EDX), however, that no graphite particles had fully transformed into carbides and that the content of Zr and Ti in the matrix were within 0.5% of the nominal composition. Thus, the carbides observed in XRD must be due to interfacial reaction between the matrix material and the reinforcement particles. Further evidence for this important observation will be provided further below.

[0041] Compression tests conducted on the composites with the lowest possible interfacial carbide formation show a large improvement in plasticity, with only a slight decrease in yield strength compared to monolithic Vit 105. Fig. 4 shows that the plastic region has strongly increased, from 3% for monolithic Vit 105 to about 7% for 3.5 vol.% graphite, 13% for 5 vol.% graphite, and 15% for 10 vol.% graphite, whereas the yield strength has decreased only slightly from 1.85 GPa for the monolithic alloy to 1.7 GPa for 3.5 vol.% graphite, 1.6 GPa for 5 vol. % graphite, and 1.5 GPa for 10 vol.% graphite reinforcement, each time at 25-44μ m particle size.

[0042] Further experiments have shown that an even higher plasticity with only a slight reduction in yield strength can be achieved by a variation in particle size. Fig. 5 show the stress-strain behavior of a composite containing 3.5 vol.% graphite particles with a particle size of 44 to 75 μm, where particular care was taken to minimize the thickness of the interfacial carbide layer. A plasticity of 18.5% in combination with a yield strength of 1.85 GPa was achieved. Further optimization appears possible.

[0043] For the samples with minimal carbide formation, the hardness (measured as Vickers Hardness HV30, see standard DIN EN ISO 6507) decreases with increasing graphite volume content, as is shown in the inset to Fig 4. Even small reinforcement volume fractions of 5% lead to significant softening of the material, and the hardness decreases by about 25% for graphite contents of ≥ 10 vol.%. On the other hand, composites displaying more carbides in XRD displayed a higher hardness of up to 550 HV30.

[0044] Figure 6 shows the yield strength and plasticity of the 5 vol.% (25-44 μm particle size), 10 vol.% (25-44 μm), and optimized (3 vol.%, 44-75 μm) graphite-reinforced BMG composites in comparison to other particle-reinforced BMG composites found in literature (accuracy of literature values: ± 10%). Apparently, the graphite-reinforced BMG composites represent a step improvement in their combination of fracture strength and plasticity.

[0045] Figures 7A - 7E show representative SEM images of fracture surfaces and particle-shear band interactions for these graphite-BMG composites (Figures 7A to 7D: 25-44 μm particle size; Figure 7E: 44-75 μm particle size). Figure 7A shows a fracture surface where a high density of vein patterns in the Vit 105 matrix is observed aroung a graphite particle: a further proof that the matrix is fully amorphous. The image in Fig. 7B shows how the graphite particle obstructs the flow of the matrix material from the top left to the bottom right during deformation (final deformation event). Figure 7C displays shear bands and steps on the outer surface of the compression samples after failure (the fracture surface is on the left side of the image), while Fig. 7D shows particle-shear band interactions on the surface of a compression sample after failure. The primary shear-band spacing around the particles is in the range of 1-5 μm, as can be concluded from Figs. 7C and 7D. Fig. 7E illustrates the high shear band density in the matrix achieved with larger graphite particles in the range of 44 to 75 μm.

Interfacial carbide formation

[0046] A further object of investigation was the effect of interfacial carbide formation on the mechanical properties. Zr being the element in the matrix with the most negative enthalpy of formation with graphite (H_{for}= -106 kJ/mol followed by -77 kJ/mol for Ti), it is expected that zirconium carbide (ZrC) forms on the surface of the graphite particles. It has previously been reported that smaller graphite particles of size below about 10 μm completely transform to ZrC in Zr based BMGs, forming an *in-situ* composite. In contrast, in the present invention, complete transformation of all graphite particles is ex-

pressly avoided.

[0047] Three samples designated as sample 1, 2 and 3 were prepared with 25-44 μm graphite particles and various amounts of interfacial carbides, induced by casting the composites at different temperatures. Samples 1, 2 and 3 were heated at a setting of 1, 2.5 and 4, respectively, on the Bühler MAM1 system (corresponding to 0.35 kW, 0.9 kW and 2.1 kW of power input).

[0048] The changes in carbide content with increasing casting temperature can be seen in the XRD scans shown in Fig. 8. The two clearly seen amorphous humps result from the glassy Vit 105 matrix. DSC also confirmed the glassy structure of the matrix. The Bragg peaks can be attributed to crystalline ZrC. While only traces of ZrC are observed in the lower scan, the ZrC content increases significantly with increasing casting temperature. The graphite peaks are not visible in the XRD scans because carbon is too light to be detected compared to the other elements present. EDX, however, proved that no graphite particles had fully transformed into carbides and that the content of Zr and Ti in the matrix were within 1% of the nominal composition. Thus, the carbides observed in XRD must be due to interfacial reaction between the matrix material and the reinforcement particles. It may be concluded that, by adjusting the power input in the final arc-melting step, it is possible to vary the carbide content of the BMG composites. Thus, in addition to the common methods of tailoring the mechanical properties of metal-matrix composites such as varying particle size, shape, hardness and volume fraction, the mechanical properties of the presently proposed Bulk Metallic Glass composites can be varied by merely varying the processing parameters.

[0049] Figure 9 shows the results of compression tests conducted on the three samples. Sample 1, with the lowest carbide content, displays the highest plasticity, whereas sample 3, where most of the carbide has formed, shows brittle fracture behavior.

[0050] Figures 10A and 10B show optical microscopy images of samples 1 and 3, respectively. In Fig. 10A, for sample 1 which was processed at the very low power setting of 0.35 kW, only a very thin interfacial reaction layer is visible, which has been broken up by polishing the sample. In Fig. 10B, for sample 3 which was processed at a high power setting of 2.1 kW, a distinctive reaction layer with a thickness of about 1.5 - 2 μm can be seen at the graphite-matrix interface. This reaction layer was still mostly intact after polishing and was thick enough to be identified as ZrC by EDX. Clearly, even in this sample, the graphite particles have not completely transformed into carbides, and a carbide layer surrounding the graphite particles is found. In the other samples, this layer is in the submicron range. The interfacial carbide phase seen in Fig. 10B appears to be responsible for the brittle fracture behavior of sample 3. On the other hand, the samples with higher carbide content display a higher hardness than the samples where only a little carbide has formed. Sample 3 in Fig. 10B, for example, displayed a hardness of 476 HV30 (comparable to the monolithic alloy), while sample 1 showed a hardness of 432 HV30.

[0051] The effect of the carbide layer on the hardness of the composites is shown in Fig. 11. Graphite-BMG composites processed at low power setting (0.35 kW) resulting in minimal carbide formation display strong softening with increasing graphite volume fraction. Samples processed at higher power setting (2.1 kW) with a thicker carbide layer display significantly higher hardness than composites with minimal carbide formation. At volume contents up to 5% the composites processed at 2.1 kW display even higher hardness than the pure matrix material.

Three-phase composites; Tribological properties

[0052] In this section, novel three-phase graphite/ZrC reinforced BMGs are discussed. The tribological properties of these BMG composites are compared to those of graphite-reinforced BMGs, as discussed above, monolithic BMG and commercial bearing steel. As a typical example, Vit 105 ($Zr_{52.5}Cu_{17.9}Ni_{14.6}Al_{10}Ti_5$) was again used as a base alloy for the BMGs; however, the invention is not limited to this base alloy.

[0053] One way of changing the tribological properties of a system is by changing the contact surface on a microscopic scale. The contact surface can be significantly influenced by adding second phase particles with different hardness than the amorphous matrix. Graphite as a reinforcement phase is promising for optimizing tribological properties because of its superlubricity and the above-discussed possibility of *in-situ* formation of very hard ZrC particles in Zr-based BMGs.

[0054] As will be seen in the following, the COF of the amorphous alloy can be decreased significantly by adding the reinforcement phases. The low COF combined with very high compressive yield strength (~1.8 GPa) of these novel composites make them potential candidates for self-lubricating friction bearing materials.

[0055] As already discussed above, it is possible to tailor the microstructure of the graphite-reinforced BMG composites by adjusting the processing parameters. Three types of BMG composites were thus produced. "Standard" graphite-reinforced BMGs as described above, which show a clean graphite-matrix interface with very little ZrC formation, was already discussed and illustrated in Fig. 10A. Increasing the processing temperature in the final casting step leads to a significant ZrC layer in the particle-matrix interface with a thickness of about 2 μm, as also discussed above and shown in Fig. 10B. If such a sample is remelted several times or smaller graphite particles are added, ZrC crystals also appear in the matrix, leading to a three-phase composite. This novel composite is illustrated in Fig. 12, where the arrow 121 indicates a graphite particle surrounded by a ZrC layer, and arrow 122 indicates a ZrC particle.

[0056] XRD scans of the three types of composites, all

displaying an amorphous background signal from the matrix, can be seen in Fig. 13. The figure shows XRD scans of the three kinds of composites, all with 7 vol.% graphite, namely (from the bottom up), Vit 105-graphite composite, composite with interfacial ZrC formation and three-phase composite with both interfacial ZrC formation and ZrC particles in the matrix. The composites with interfacial ZrC and additionally ZrC in the matrix both show ZrC peaks of similar intensity compared to the standard graphite-reinforced BMG sample which displays almost no carbide formation. Samples displaying no carbide formation and the three-phase composites were used for tribological testing.

[0057] Fig. 14 illustrates the setup used for tribological testing. A steel ball is moved in circles over the sample surface with a predetermined pressing force (load), thus creating a wear track.

[0058] An SEM image of a sample containing 8 vol.% graphite is shown in Fig. 15 after tribological testing. This SEM image shows an overview of wear tracks made at different parameters, where the first parameter indicates the vertical load and the second parameter indicates the number of revolutions of the steel ball. A homogeneous particle distribution is visible, which was found in all composites.

[0059] XRD scans performed before and after tribological testing on the sample plates of both types of BMG composites displayed no significant changes, as can be seen in Fig. 16. One must however consider that only about 5% of the sample surface was affected by the tribology tests.

[0060] A comparison of coefficient of friction (COF) and wear trace depth for monolithic samples and composites in 1000 revolution tests conducted at a load of 1 N was performed. Amorphous Vit 105 displayed a much higher COF and much higher fluctuations of COF than the fully crystallized alloy. The COF of the amorphous sample dropped slightly until it stabilized after about 300 revolutions, whereas the crystalline sample displayed a constant COF throughout the test. All the composites displayed two significant levels of COF. At the beginning of the test, they showed a stable COF which is significantly lower than in the monolithic matrix material. After > 100 revolutions they jumped to an even lower level of COF where some composites stay whereas other make jumps back up to the higher level where they stay for < 100 revolutions. This behavior was especially prominent in samples with significant ZrC content. It was also found that a higher reinforcement content led to less fluctuations in COF. All samples tested for 1000 revolutions showed a more or less linear increase in wear track depth except for the amorphous monolithic Vit 105 which exhibited significant pin lifting.

[0061] At a force of 1 N the amorphous monolithic alloy showed a COF of about 0.8 which is comparable to the value measured for the hardened bearing steel (0.78). Crystallized Vit 105 displayed a COF of 0.6. It was found that the reinforcement of the monolithic glass with very low volume contents of graphite leads to a significant decrease in COF as can be seen in Fig. 17. Composites with additional ZrC reinforcement show an even larger decrease in COF especially in the lower COF regime seen in the 1000 revolution runs. No significant difference in the effect of graphite reinforcement was found for tests run at a 5 N load for 100 revolutions; however, ZrC did not lead to quite as large of a decrease in COF as for samples run at a 1 N load.

[0062] Some shear bands were found at the edge of the wear traces after 1000 revolutions at 1 N. The shear bands run about 25° to the sliding direction and give evidence for high enough stresses to lead to inhomogeneous flow. In some composite samples, smeared matrix material was found in the wear trace. This is expected to come from deformation in the undercooled liquid region.

[0063] In general very little smearing of graphite was observed in the composite samples. It was found by SEM investigation that whole graphite particles were ripped out of the matrix during the wear tests between 100 and 1000 revolutions. Composites samples containing ZrC showed several channels in their wear tracks. The depth of the channels was estimated to be about 3 μm. On the steel tip of a composite sample containing ZrC, lots of small particles with a particle size between 50 and 500 nm were found on the surface, which are thought to be ZrC debris.

[0064] Comparing the width of the wear tracks and pin depths gives a very qualitative approximation of the wear rate. The thinnest wear track after 1000 revolutions at 1 N was found for crystalline Vit 105, the thickest for the hardened steel with about 50 μm and 200 μm respectively. No significant difference was seen between the amorphous alloy and the composites, which all displayed trace widths of about 120 μm. The depths of the wear tracks are difficult to compare because of the observed pin lifting phenomena. It was found that the wear tracks of the BMG composites after 1000 revolutions at a load of 1 N are slightly less deep than in the bearing steel. The depths and widths of the wear tracks do not correlate with the hardness of the monolithic materials which are 846 HV for the bearing steel, 547 HV and 478 HV for crystalline and amorphous Vit 105 respectively.

Discussion

[0065] In discussing the above results, it should first be emphasized that a homogeneous particle distribution, as shown in Fig. 1, might have been only achievable because of the good wetting behavior between graphite and Vit 105 and due to the multiple-step induction mixing procedure proposed. Preliminary attempts to produce composites with non-wetting particles indeed led to particle agglomerations. As for the DSC results (Fig. 2), the addition of graphite apparently improved the thermal stability of the composites compared to the monolithic alloy, such that these composites may also be used for superplastic forging. The phenomenon of improved thermal

stability was also observed for SiC reinforcement particles in a Zr-based BMG composite. The effect may be due either to the change in thermal conductivity compared to the monolithic BMG or because of a slight shift in matrix composition resulting from the interfacial carbide reaction. The latter may also be responsible for the slight change in crystallization behavior.

[0066] The combination of fracture strength and plasticity found in the present composites appears to be the highest ever recorded for foreign-particle-reinforced BMGs, as is shown in Fig. 6. While similar plasticity has been seen in 50% Nb-reinforced Zr-based BMGs, in those alloys the yield strength dropped drastically to 30% of the strength of the monolithic alloy due to the high reinforcement volume fraction deployed. Our key to success was the use of "soft" reinforcement particles, i.e. a reinforcement material with a much lower Young's modulus (ca. 15 GPa in graphite) than that of the Vit 105 matrix (Young's modulus, $E \approx 100$ GPa). In contrast, all the other reinforcement materials shown in Fig. 6 have a higher Young's modulus than the matrix material: for the refractory metals Nb, Ta, and Mo, for example, *E* ranges from 105 to 327 GPa. The lower Young's modulus of the graphite leads to local compressive stress concentrations in the matrix material close to the particle-matrix interface, while tensile stresses in the matrix are expected to occur for "hard" particle reinforcement. Thus, on the one hand graphite may act as a typical reinforcement particle, splitting shear bands (such splitting and the particle-shear band interaction is shown in Figs. 7C and 7D); on the other hand, the graphite particles are expected to halt the propagation of shear bands by reducing the stress at their tips when they run onto the soft material. This is actually shown in Figs. 7A and 7B, where the reinforcement particle clearly hinders the matrix flow during deformation. Because of their low strength the graphite particles may act in a way similar to pores in amorphous alloys. During compression testing the first shear band may be initiated as soon as the stress in the "soft" particle (or pore) reaches a critical value. After initiation of this shear band the stress around this particle decreases, while other shear bands are initiated at the particles which reach critical stress concentrations. Thus, multiple shear bands nucleate, run through the material and cross, and thus hinder, each other - which leads to enhanced plasticity. These results - enhanced plasticity and strength in combination with reproducibility of microstructure - are expected to have a significant influence on the field of bulk metallic glass strengthening, as did earlier results in the field of nanostructured metals. There, an improvement was achieved with the development of a two-phase material of micrometer-sized grains embedded in a matrix of grains with sizes < 300 nm.

[0067] Apparently the combination of the above mentioned effects (shear-band splitting, impairment of propagation, and shear-band initiation) generates a great increase in plasticity at very low graphite content, which in turn leads to only minimal decrease in yield strength compared to the monolithic alloy. The regions around the particles display a very small shear-band spacing in the micrometer or even sub-micrometer range (Figs. 7A to 7E), in contrast to what has been reported for monolithic Zr-based BMGs. Indeed, a direct correlation between reduced shear-band spacing and enhanced plasticity has been reported for metallic glass ribbons of varying thickness and BMG composites. As can be seen in Fig. 4, there is no significant plasticity benefit if the graphite content is increased from 5 to 10 vol.%. Once the inter-particle distance is small enough to generate a homogeneous high shear-band density in the matrix during deformation, more reinforcement particles will not further improve plasticity in any significant way. Indeed, doubling the reinforcement concentration will reduce the inter-partide distance by only about 1/3.

[0068] The foreign-particle reinforced composites also provide the advantage that their mechanical properties can be tailored by tuning the carbide formation. As can be seen in the XRD scans of Figs. 3 and 8, the amount of graphite that transforms into ZrC can be adjusted by altering the casting temperature. To prevent brittle fracture behavior, however, it may be beneficial to keep the carbide content fairly low, and the ZrC content only appears dominant in the XRD scans because of Zr's high atomic mass. On the other hand, EDX shows that the graphite particles did not transform fully into carbides, and the optical microscopy image in Figs. 10A and 10B provides evidence that only an interfacial carbide layer formed even at a high casting temperature. Indeed, if much carbide had formed in the composites, the matrix composition would have shifted and glass-forming ability would have decreased. The softening of the composite with increasing reinforcement volume fraction (inset to Fig. 4) also suggests that only a very small fraction of the graphite reacted to carbide. A similar minor carbide formation in the matrix-particle interface has previously also been observed in carbon-fiber-reinforced Zr-based BMG composites. In contrast, however, most other studies have shown a complete transformation of the graphite particles into ZrC. For example, carbon or graphite particles of ≤ 10 μm have been used to process BMG-ZrC composites *in situ,* and a distinct increase in hardness has been observed. This apparent contradiction of carbide formation, or lack of it, can be explained by the fact that larger graphite particles of ≥ 25 μm were used in this study, and special care was taken to heat moderately during processing.

[0069] In the present case the carbides start growing in the matrix-particle interface forming a hard shell around the graphite particles. Interfacial carbide formation is favored because of the short diffusion paths necessary. The formed ZrC layer acts as a diffusion barrier and slows the carbide formation in the interface controlling the reaction. It is expected that strong stirring of the melt could lead to complete reaction of graphite to ZrC because the evolving ZrC would be separated from the graphite allowing further carbide reaction in the interface.

The thin interfacial carbide layer leads to a significant increase in hardness compared to the standard graphite composites. If the graphite particles are considered as spheres of 35 μm and the graphite layer as an interfacial layer of 1.5 μm, composites containing 5 vol.% graphite contain less than 0.7 vol.% ZrC. Due to this layer, an increase in hardness of about 16% is observed, compared to the composite with 5 vol.% graphite and minimal carbide formation. This phenomenon cannot be explained by Ashby's rules of mixing because of the geometrical particularities of the carbide surrounding the graphite particles. If the graphite particle with the hard carbide shell around it is considered as a monolithic reinforcement particle, it will display similar mechanical properties like a hard-boiled egg. At low stress, it will be very stiff. If higher stress is applied, the shell will break and it will act like a soft particle. The stress value necessary to "crack the shell" is of course determined by the thickness of the carbide layer but also by the shape and size of the graphite particle. At very low reinforcement, graphite leads to a strong decrease in hardness whereas the composites with the carbide layers show a slight increase, as one would expect for a matrix reinforced with hard particles. At higher reinforcement contents, the hardness of the composites with an interfacial carbide layer also starts to decrease and the soft graphite seems to become dominant. It is expected that when hardness testing is conducted on samples with low graphite volume content the hard particles are pushed into the soft matrix relieving stress on the particles, whereas at high volume contents they hinder each other and are exposed to enough stress to crack the carbide shells and the graphite becomes dominant.

[0070] The thickness of the interfacial carbide layer also has a significant influence on the stress-strain behavior of the composites. Soft graphite particles with a low Young's modulus are favorable in achieving high plasticity in compression. The thicker the interfacial carbide layer around a graphite particle, the more it will act like a hard ceramic particle instead of a soft graphite particle. As apparent from Fig. 9, the thicker the interfacial carbide layer, the more brittle the material becomes. The carbide layer that has a Young's modulus of about 400 GPa compared to 100 GPa of the matrix material leads to tensile stress concentrations close to the particle matrix interfaces in such a way that propagating shear bands are led around the reinforcement particles, hindering shear band-particle interaction. In addition, the high hardness of the carbide layer (about 2500 HV compared to 15 HV of graphite) hinders the absorption of approaching shear bands but deflects them, leading to fracture on one or few bands.

[0071] If plasticity is desired to be maximized, the carbide layer should therefore be kept as thin as possible. Even in samples processed at the lowest possible energy input where casting is still possible, some ZrC was detected in XRD. While it might thus be impossible to fully eliminate the carbide layer, it is still possible to weaken the strength of a carbide shell by increasing the particle size. If once again the particles are approximated as a soft sphere with a hard shell around it, a shell of the same thickness will carry less load if the sphere is larger. As can be seen in Fig. 5, larger graphite particles lead to very high plasticity at low reinforcement volume fractions. Samples with 3.5 vol.% particles of 25-44 μm display only about 7% plasticity compared to up to 18.5% with 45-75 μm particles. This low volume content of graphite leads to only a slight reduction of yield strength compared to the monolithic alloy.

[0072] It was also shown above that graphite reinforcement of Vit 105 leads to a significant change in tribological behavior. The reinforcement reduces stick-slip and leads to a significant decrease in COF. Graphite is known to lower the COF of tribological partners in metallic and polymer-based materials. In metallic systems, graphite sticks especially well on oxidized surfaces (as are present on the surface of Zr-based BMGs), which, on a microscopic scale, can lead to graphite sliding on graphite, which displays a very low COF. In addition it was also observed in the present study that debris was pushed into the soft graphite particles or the holes from ripped out particles, which is expected to lead to less abrasive wear and additionally lower the COF.

[0073] It was further observed that the newly developed three-phase composite shown in Fig. 12 resulted if samples were remelted and suction cast multiple times. This probably led to ZrC breaking off the graphite particles and distributing itself in the melt. An even more prominent drop in the COF was found for these three-phase composites especially in their lower regime of COF (see Fig. 17).

[0074] The jumps in COF observed in the composites containing ZrC are clear evidence for two different sliding mechanisms. In the regime of high COF strong fluctuations of COF are observed as is common for the monolithic matrix material and also composites reinforced only with graphite. This leads to expect a similar wear mechanism as in the graphite-reinforced composites with the exception of the effect of the hard particles in the matrix. However, once the COF drops to the lower regime the fluctuations of COF also decrease drastically, which, in combination with the observed channel-like morphology of the wear track, gives evidence for a new sliding mechanism.

[0075] The channel-like morphology of the wear tracks observed in composites with *in situ* formed ZrC stands in contrast to the relatively smooth wear tracks found in graphite-reinforced Vit 105 or the monolithic matrix material. Due to the very high strain rates achieved on the micro-scale during sliding ($\sim 10^5\ s^{-1}$) it is unlikely that the channels are formed by inhomogeneous deformation of the matrix material but much more by local abrasion of the matrix material by ZrC debris. Very small particles which are expected to be ZrC debris were found on the steel ball used for such tests. It is expected that larger ones were also present but fell off due to their lower sur-

face-to-weight ratio. Once a shallow channel has formed, debris will remain in the channel and lead to local abrasion deepening it.

[0076] These findings indicate that the wear behavior of this three-phase composite is based mainly on the geometrical particularities of the wear traces. A possible explanation for the observed tribological particularities may be that during the low regime of the COF debris is pushed in front of the steel ball, leading to the observed channels in the wear tracks. A steady state is achieved where the steel ball slides on top of the channels, leading to a slightly lower COF than in composites reinforced only with graphite, due to the smaller contact surface leading to less adhesive friction. The transition from the high to the low regime of COF takes place within very few revolutions and is accompanied by a significant increase in pin height of about 2 μm. This is thought to be due to the channels filling up with debris and the steel ball being lifted onto the debris and sliding on top of it. The debris, which seems to be quite round, is thought to reduce the frictional forces by rolling underneath the steel ball in the wear channels. Jumps back up to the higher regime of COF may take place when a graphite particle is ripped out of the wear track and large amounts of debris is pushed into the hole which leads to the ball dropping back down onto the channel walls and sliding on them.

[0077] The fact that very low reinforcement contents are sufficient for lowering the COF in both composites gives further evidence that the mechanisms are not based on the static pairing of the two materials but much more on the influence of debris on the dynamic contact during sliding. In the one case graphite acts as a lubricant and debris trap, in the other, ZrC leads to channel formation changing the topography of the wear track. Especially once the wear track has reached a certain depth, debris will stay in the track and not be pushed out over the edge.

[0078] In contrast to previous accounts, no hint for crystallization of the wear track or debris during wear was found; however, some smearing of matrix material was observed. This smearing is expected to take place in the undercooled liquid region, which is quite large in the matrix material. Due to the very low sliding speed the smeared material is probably cooled by heat transfer to the bulk of the sample before the next revolution takes place. This cooling is thought to be fast enough to hinder local crystallization. The local stress on the sample during the tribology tests can be quite large. If one considers the contact surface to be a circle with the diameter of the wear track (120 μm) the global stress would be about 90 MPa at a 1 N load. If one, however, considers that very small particles of hard debris might be between the ball and the sample the contact surface will decrease significantly leading to very high local stress which could easily be above the flow stress of the matrix material (about 1.9 GPa) which would also explain the observed local shear banding on the edge of the wear track.

[0079] As far as wear rate is concerned, the present observations are very qualitative. However, the width of the wear tracks and the measured depths of the wear traces give evidence that the wear rate of the composites is lower than in amorphous Vit 105 and commercial bearing steel in the used testing set up. This is thought to be at least partially due to the self-lubricating effect of graphite and the holes of tom out graphite particles acting as traps for debris, both leading to less abrasive wear.

Conclusion

[0080] In conclusion, the BMG-graphite composites developed in this study constitute a very promising material for structural applications due to their high plasticity, comparable to that of crystalline alloys, combined with the high yield strength typical of metallic glasses. The matrix-particle interface, particularly its hardness, has a major influence on the mechanical properties of these composites. Since the microstructure of these foreign-particle reinforced composites can be tailored and easily reproduced for specific applications, one may expect that these new composites will have a great impact on research efforts in the entire field of amorphous structural materials.

[0081] Furthermore, the tribological properties of graphite-reinforced and of a newly developed graphite- and carbide-reinforced BMGs were compared to those of amorphous and crystalline alloys as well as bearing steel. It was found that graphite and especially carbide reinforcement leads to a significant decrease in COF. The carbide-containing composites displayed two regimes of COF. The very low COF found in the lower regime is thought to be due to the geometry of the wear tracks formed by carbide particles. In this wear regime the COF is up to four times lower than in the monolithic alloy. Crystallization of the wear tracks or debris after tribological testing was not observed. A qualitative comparison of the wear rate gives evidence that the newly developed composites may show even lower wear rates than the 100Cr6 bearing steel used as a reference material. These tribological properties combined with the high yield strength of the composites make them an interesting candidate for a dry frictional bearing material.

[0082] While the above examples related to composites based on Vit 105, it is to be expected that similar results can be achieved also with composites based on BMGs with a different composition, and the invention is in no way limited to composites based on Vit 105. While a homogeneous particle distribution is more easily achieved if the wettability of the particle surface by the matrix alloy is good, composites can also be produced for which wettability is poor. Likewise, it is not necessary that a reaction can occur between the matrix alloy and graphite. However, the above-described experiments suggest that Zr-based glass-forming alloys are particularly good matrix materials for the composites of the present invention.

Methods

(a) Sample Preparation

[0083] Pre-alloys with the atomic composition $Zr_{52.5}Cu_{17.9}Ni_{14.6}Al_{10}Ti_5$ (Vit 105) were prepared in a Bühler AM system by arc melting the high-purity elements (> 99.95%) in a 300 mbar Ar 6.0 atmosphere and casting the molten alloy ingot into a Cu mould of 13 mm in diameter and 40 mm in length. The subsequent composite preparation took place in a 1200 mbar Ar 6.0 atmosphere. 2-20 vol.% conducting-grade graphite with a particle size of 25-44 μm or 44-75 μm was mixed with the matrix material by induction melting of the alloy on top of the graphite powder in a water-cooled silver boat. After the powder was picked up the sample was remelted in the silver boat to achieve a homogeneous particle distribution. The crystalline composites were then suction-cast into 3 mm rods with a length of 30 mm (for compression testing, thermophysical characterization and imaging) or into 2 mm x 7 mm x 30 mm plates (for tribology measurements) in a Bühler MAM1 arc melter. 5-mm-long slices were cut from the 3 mm rods for compression testing. Thinner slices were cut for thermophysical investigation. Tribology samples were first ground and then polished with a 0.05 μm Al_2O_3 dispersion.

[0084] Standard samples were cast at an arc power setting of 1 (corresponding to 0.35 kW power input), while a setting of 2.5 (1 kW) and 4 (2.1 kW) was used to induce interfacial ZrC formation. If necessary, samples were remelted several times to initiate a stronger carbide formation.

[0085] Monolithic BMG samples were prepared without the induction mixing step, one sample was fully crystallized by annealing at 430°C for 75 min. Hardened 100Cr6 bearing steel was used as a reference sample for tribological testing.

(b) Structural and thermophysical characterization

[0086] XRD was performed on polished samples with a PANalytical X'Pert diffractometer using Cu-K_α radiation. A Seiko DSC 220CU system and a Setaram Labsys system were used for calorimetric analysis. Calorimetric measurements were performed using a sample weight of approximately 20 mg at a heating rate of 20 K/min. A CamScan scanning electron microscope (SEM) equipped with a Noran Energy Dispersive X-ray (EDX) detector was used for elemental analysis. Samples for optical microscopy were polished with a 0.05 μm Al_2O_3 suspension and etched with a solution of 30 ml HNO_3 in 70 ml of distilled water. A Reichert-Jung Polyvar Met microscope combined with a Leica camera was used to create the optical microscopy images.

(c) Mechanical characterization

[0087] Hardness measurements were performed on a Gnehm Brickers 220 instrument at a setting of HV 30 with an impression time of 6 s. Compression tests were conducted on a Schenk Trebel tensile tester combined with Merlin software at a strain rate of 10^{-3} s^{-1}. A high-resolution Zeiss Gemini 1530 FEG scanning electron microscope was used for microstructure investigation.

(d) Tribological characterization

[0088] The tribological properties of the material were investigated on a CETR microtribometer, where the sample was paired against a bearing steel ball with a diameter of 2 mm at a constant sliding speed of 100 mm/min without lubrication. All tests were run at room temperature and a relative humidity of about 40%. After the ball was run in for 100 revolutions at a 5 N load a first test was performed with the same parameters, followed by 100, 10 and 1000 (not performed on all samples) revolution tests at a 1 N load. The ball was run in at a radius of 2.9 mm and the radius was reduced by 0.4 mm for each of the following tests. The high regime of the COF was determined by linear approximation of the force data obtained in the 100 revolution tests. In the steel sample the 1000 revolution data was used because COF was not yet in equilibrium after 100 revolutions due to the oxide layer. In samples displaying two regimes of COF in the 1000 revolution tests, the lower regime of COF was determined by averaging the values of the lower shelves. Graphite volume content of the tribology surfaces was determined by investigation of optical micrographs with Leica QWin software.

List of abbreviations

[0089]

BMG	bulk metallic glass
COF	coefficient of friction
DSC	differential scanning calorimetry
EDX	energy-dispersive X-ray diffraction
XRD	X-ray diffraction
SEM	scanning electron microscopy
HV30	Vickers hardness, measured at 30 N impression force

Claims

1. A composite material comprising

- an amorphous first phase forming a continuous matrix, said first phase consisting of an alloy; and
- a second phase embedded in said matrix, said second phase comprising graphite particles having a size in the range between 1 and 100 micrometers, wherein said second phase occupies between 3 volume percent and 20 volume

percent of said composite material.

2. The composite material according to claim 1, wherein said graphite particles have a size in the range between 25 and 75 micrometers.

3. The composite material according to one of the preceding claims,
wherein said second phase is selected such that, under compressive deformation of said composite material up to yield, it induces a distribution of shear bands spaced apart by less than about 5 micrometers around said graphite particles.

4. The composite material according to one of the preceding claims,
wherein said alloy of the first phase, in the liquid state, is capable of wetting said second phase.

5. The composite material according to one of the preceding claims,
wherein said alloy comprises at least about 40 atomic percent of a metal having a negative enthalpy of formation for the reaction with graphite to form a metal carbide.

6. The composite material according to one of the preceding claims, wherein said alloy comprises at least about 40 atomic percent of zirconium.

7. The composite material according to one of the preceding claims, wherein said alloy consists of $Zr_{52.5}Cu_{17.9}NG_{14.6}Al_{10}Tims_5$.

8. The composite material according to one of the preceding claims, wherein at least a fraction of said graphite particles in said second phase have a core consisting of graphite and a surface layer comprising at least one metal carbide.

9. The composite material according to claim 8, wherein said surface layer has a thickness of at least 100 nanometers.

10. The composite material according to claim 8 or 9, wherein said graphite particles have a size of at least about 25 micrometers.

11. The composite material according to one of claims 8 to 10, wherein said surface layer comprises at least one metal carbide formed *in situ* by a reaction of graphite with said alloy.

12. The composite material according to one of claims 8 to 11, wherein said surface layer consists of zirconium carbide.

13. The composite material according to one of the preceding claims, further comprising a third phase embedded in said matrix, wherein said third phase comprises crystalline particles.

14. The composite material of claim 13, wherein said third phase comprises crystalline particles composed of the same elements as said alloy of the first phase.

15. The composite material of claim 13, wherein said third phase comprises carbide particles.

16. The composite material according to claim 15, wherein said carbide particles comprise at least one metal carbide formed *in situ* by a reaction of graphite with said alloy.

17. The composite material according to claim 15 or 16, wherein said carbide particles consist of zirconium carbide.

18. The composite material according to one of claims 15 to 17, wherein
said carbide particles have a size of less than or equal to about 10 micrometers.

19. Use of a composite material according to one of claims 1 to 18 for manufacturing an object for use in a device selected from: a frictional bearing, a joint, a spring.

20. A method for manufacturing a composite material, said method comprising:

- heating an alloy above its liquidus temperature to form a liquid alloy;
- dispersing graphite powder in the liquid alloy to form a finely dispersed mixture;
- cooling the mixture below its glass transition temperature sufficiently rapidly for forming a composite material comprising an amorphous first phase forming a continuous alloy matrix and a second phase embedded in said matrix, said second phase comprising graphite particles having a size in the range between 1 and 100 micrometers, wherein said second phase occupies between 3 volume percent and 20 volume percent of said composite material.

21. The method of claim 20, wherein said alloy is heated above its liquidus temperature by induction melting on top of said graphite powder.

22. The method of claim 20 or 21, wherein said mixture is remelted at least once for a time sufficiently long for a distinct carbide layer to form on the surface of said graphite particles.

23. The method of one of claims 20 to 22, wherein said mixture is remelted at least once for a time sufficiently long for a fraction of said graphite particles reacting with at least one metal component of said alloy to form metal carbide particles.

Patentansprüche

1. Verbundmaterial, aufweisend:

- eine amorphe erste Phase, die eine kontinuierliche Matrix bildet, wobei die erste Phase aus einer Legierung besteht; und
- eine zweite Phase, die in der Matrix eingebettet ist, wobei die zweite Phase Graphitteilchen mit einer Grösse im Bereich zwischen 1 und 100 Mikrometer enthält, wobei die zweite Phase zwischen 3 Volumenprozent und 20 Volumenprozent des Verbundmaterials einnimmt.

2. Verbundmaterial nach Anspruch 1, wobei die Graphitteilchen eine Grösse zwischen 25 und 75 Mikrometer aufweisen.

3. Verbundmaterial nach einem der vorhergehenden Ansprüche, wobei die zweite Phase derart gewählt ist, dass sie unter kompressiver Deformation des Verbundmaterials bis zum Fliessen eine Verteilung von Scherbändern induziert, wobei um die Graphitteilchen herum die Scherbänder um weniger als ungefähr 5 Mikrometer voneinander entfernt sind.

4. Verbundmaterial nach einem der vorhergehenden Ansprüche, wobei die Legierung der ersten Phase, wenn sie sich im flüssigen Zustand befindet, in der Lage ist, die zweite Phase zu benetzen.

5. Verbundmaterial nach einem der vorhergehenden Ansprüche, wobei die Legierung mindestens ca. 40 Atom-Prozent eines Metalls enthält, welches eine negative Bildungsenthalpie für die Reaktion mit Graphit zur Bildung eines Metallkarbids aufweist.

6. Verbundmaterial nach einem der vorhergehenden Ansprüche, wobei die Legierung mindestens ca. 40 Atom-Prozent Zirkonium enthält.

7. Verbundmaterial nach einem der vorhergehenden Ansprüche, wobei die Legierung aus $Zr_{52.5}Cu_{17.9}Ni_{14.6}Al_{10}Ti_5$ besteht.

8. Verbundmaterial nach einem der vorhergehenden Ansprüche, wobei zumindest ein Teil der Graphitteilchen in der zweiten Phase einen Kern aufweisen, der aus Graphit besteht, sowie eine Oberflächenschicht aufweisen, die mindestens ein Metallkarbid enthält.

9. Verbundmaterial nach Anspruch 8, wobei die Oberflächenschicht eine Dicke von mindestens 100 Nanometer aufweist.

10. Verbundmaterial nach Anspruch 8 oder 9, wobei die Graphitteilchen eine Grösse von mindestens ca. 25 Mikrometer aufweisen.

11. Verbundmaterial nach einem der Ansprüche 8 bis 10, wobei die Oberflächenschicht mindestens ein Metallkarbid enthält, dass *in situ* durch eine Reaktion von Graphit mit der Legierung gebildet wurde.

12. Verbundmaterial nach einem der Ansprüche 8 bis 11, wobei die Oberflächenschicht aus Zirkoniumkarbid besteht.

13. Verbundmaterial nach einem der vorhergehenden Ansprüche, welches ausserdem eine dritte Phase aufweist, die in der Matrix eingebettet ist, wobei die dritte Phase kristalline Teilchen enthält.

14. Verbundmaterial nach Anspruch 13, wobei die dritte Phase kristalline Teilchen enthält, die aus denselben Elementen wie die Legierung der ersten Phase zusammengesetzt sind.

15. Verbundmaterial nach Anspruch 13, wobei die dritte Phase Karbidteilchen enthält.

16. Verbundmaterial nach Anspruch 15, wobei die Karbidteilchen mindestens ein Metallkarbid enthalten, dass *in situ* durch eine Reaktion von Graphit mit der Legierung gebildet wurde.

17. Verbundmaterial nach Anspruch 15 oder 16, wobei die Karbidteilchen aus Zirkoniumkarbid bestehen.

18. Verbundmaterial nach einem der Ansprüche 15 bis 17, wobei die Karbidteilchen eine Grösse von kleiner oder gleich 10 Mikrometer aufweisen.

19. Verwendung eines Verbundmaterials nach einem der Ansprüche 1 bis 18 zur Herstellung eines Objektes zur Verwendung in einer Vorrichtung ausgewählt aus: ein Reiblager, ein Gelenk, eine Feder.

20. Verfahren zur Herstellung eines Verbundmaterials, aufweisend:

- Erhitzen einer Legierung über ihre Liquidus-Temperatur, um eine flüssige Legierung zu bilden;
- Dispergieren von Graphitpulver in der flüssigen Legierung, um eine fein dispergierte Mischung zu bilden;
- Abkühlen der Mischung unter ihre Glasübergangstemperatur, wobei dies genügend schnell

erfolgt, um ein Verbundmaterial zu bilden, welches eine amorphe erste Phase, die eine kontinuierliche Legierungsmatrix bildet, und eine zweite Phase, die in der Matrix eingebettet ist und Graphitteilchen mit einer Grösse im Bereich zwischen 1 und 100 Mikrometer enthält, aufweist, wobei die zweite Phase zwischen 3 Volumenprozent und 20 Volumenprozent des Verbundmaterials einnimmt.

21. Verfahren nach Anspruch 20, wobei die Legierung durch Induktionsschmelzen über dem Graphitpulver über ihre Liquidus-Temperatur erhitzt wird.

22. Verfahren nach Anspruch 20 oder 21, wobei die Mischung mindestens einmal umgeschmolzen wird, und zwar für eine genügend lange Zeit, damit sich eine wahrnehmbare Karbidschicht auf der Oberfläche der Graphitteilchen bildet.

23. Verfahren nach einem der Ansprüche 20 bis 22, wobei die Mischung mindestens einmal umgeschmolzen wird, und zwar für eine genügend lange Zeit, damit ein Teil der Graphitteilchen mit mindestens einer Metallkomponente der Legierung reagiert, um Metallkarbid-Teilchen zu bilden.

Revendications

1. Matériau composite comprenant

- une première phase amorphe formant une matrice continue, ladite première phase consistant en un alliage ; et
- une deuxième phase noyée dans ladite matrice, ladite deuxième phase comprenant des particules de graphite ayant une taille dans la gamme comprise entre 1 et 100 micromètres, ladite deuxième phase occupant entre 3 pour cent en volume et 20 pour cent en volume dudit matériau composite.

2. Matériau composite selon la revendication 1, dans lequel lesdites particules de graphite ont une taille dans la gamme comprise entre 25 et 75 micromètres.

3. Matériau composite selon l'une quelconque des revendications précédentes, dans lequel ladite deuxième phase est choisie de telle sorte que, sous déformation par compression dudit matériau composite jusqu'à la limite élastique, elle induit une distribution de bandes de cisaillement espacées de moins d'environ 5 micromètres autour desdites particules de graphite.

4. Matériau composite selon l'une quelconque des revendications précédentes, dans lequel ledit alliage de la première phase, à l'état liquide, est capable de mouiller ladite deuxième phase.

5. Matériau composite selon l'une quelconque des revendications précédentes, dans lequel ledit alliage comprend au moins environ 40 pour cent en atomes d'un métal présentant une enthalpie de formation négative dans une réaction avec le graphite pour former un carbure métallique.

6. Matériau composite selon l'une quelconque des revendications précédentes, dans lequel ledit alliage comprend au moins environ 40 pour cent en atomes de zirconium.

7. Matériau composite selon l'une quelconque des revendications précédentes, dans lequel ledit alliage consiste en $Zr_{52,5}Cu_{17,9}Ni_{14,6}Al_{10}Ti_5$.

8. Matériau composite selon l'une quelconque des revendications précédentes, dans lequel au moins une fraction desdites particules de graphite dans ladite deuxième phase possède un coeur consistant en du graphite et une couche de surface comprenant au moins un carbure métallique.

9. Matériau composite selon la revendication 8, dans lequel ladite couche de surface a une épaisseur d'au moins 100 nanomètres.

10. Matériau composite selon la revendication 8 ou 9, dans lequel lesdites particules de graphite ont une taille d'au moins environ 25 micromètres.

11. Matériau composite selon l'une quelconque des revendications 8 à 10, dans lequel ladite couche de surface comprend au moins un carbure métallique formé *in situ* par une réaction du graphite avec ledit alliage.

12. Matériau composite selon l'une quelconque des revendications 8 à 11, dans lequel ladite couche de surface consiste en du carbure de zirconium.

13. Matériau composite selon l'une quelconque des revendications précédentes, comprenant en outre une troisième phase noyée dans ladite matrice, ladite troisième phase comprenant des particules cristallines.

14. Matériau composite selon la revendication 13, dans lequel ladite troisième phase comprend des particules cristallines composées des mêmes éléments que ledit alliage de la première phase.

15. Matériau composite selon la revendication 13, dans lequel ladite troisième phase comprend des particu-

les de carbure.

16. Matériau composite selon la revendication 15, dans lequel lesdites particules de carbure comprennent au moins un carbure métallique formé *in situ* par une réaction du graphite avec ledit alliage.

17. Matériau composite selon la revendication 15 ou 16, dans lequel lesdites particules de carbure consistent en du carbure de zirconium.

18. Matériau composite selon l'une quelconque des revendications 15 à 17, dans lequel lesdites particules de carbure ont une taille inférieure ou égale à environ 10 micromètres.

19. Utilisation d'un matériau composite selon l'une quelconque des revendications 1 à 18 pour la fabrication d'un objet pour utilisation dans un dispositif choisi parmi un palier à friction, un joint et un ressort.

20. Procédé de fabrication d'un matériau composite, ledit procédé comprenant :

- le chauffage d'un alliage au-dessus de sa température de liquidus pour former un alliage liquide ;
- la dispersion d'une poudre de graphite dans l'alliage liquide pour former un mélange finement dispersé ;
- le refroidissement du mélange en dessous de sa température de transition vitreuse, suffisamment rapidement pour former un matériau composite comprenant une première phase amorphe formant une matrice en alliage continue et une deuxième phase noyée dans ladite matrice, ladite deuxième phase comprenant des particules de graphite ayant une taille dans la gamme comprise entre 1 et 100 micromètres, ladite deuxième phase occupant entre 3 pour cent en volume et 20 pour cent en volume dudit matériau composite.

21. Procédé selon la revendication 20, dans lequel ledit alliage est chauffé au-dessus de sa température de liquidus par fusion par induction sur ladite poudre de graphite.

22. Procédé selon la revendication 20 ou 21, dans lequel ledit mélange est refondu au moins une fois pendant un temps suffisamment long pour qu'une couche de carbure distincte se forme sur la surface desdites particules de graphite.

23. Procédé selon l'une quelconque des revendications 20 à 22, dans lequel ledit mélange est refondu au moins une fois pendant un temps suffisamment long pour qu'une fraction desdites particules de graphite réagisse avec au moins un composant métallique dudit alliage pour former des particules de carbure métallique.

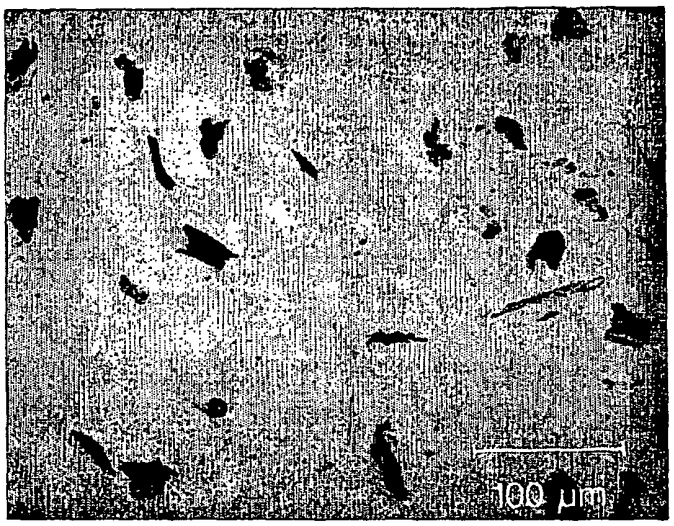

100 µm

FIG. 1

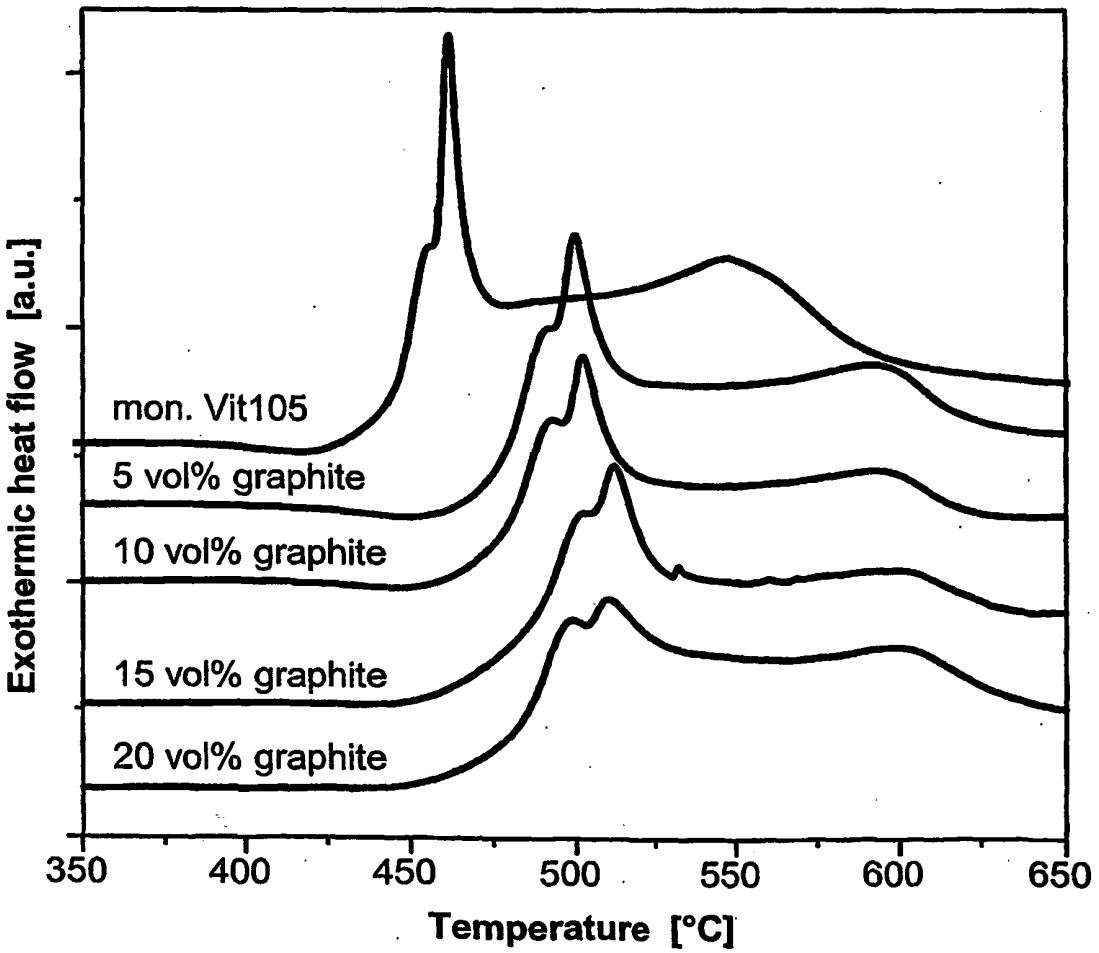

Exothermic heat flow [a.u.]
mon. Vit105
5 vol% graphite
10 vol% graphite
15 vol% graphite
20 vol% graphite
350
400
450
500
550
600
650
Temperature [°C]

FIG. 2

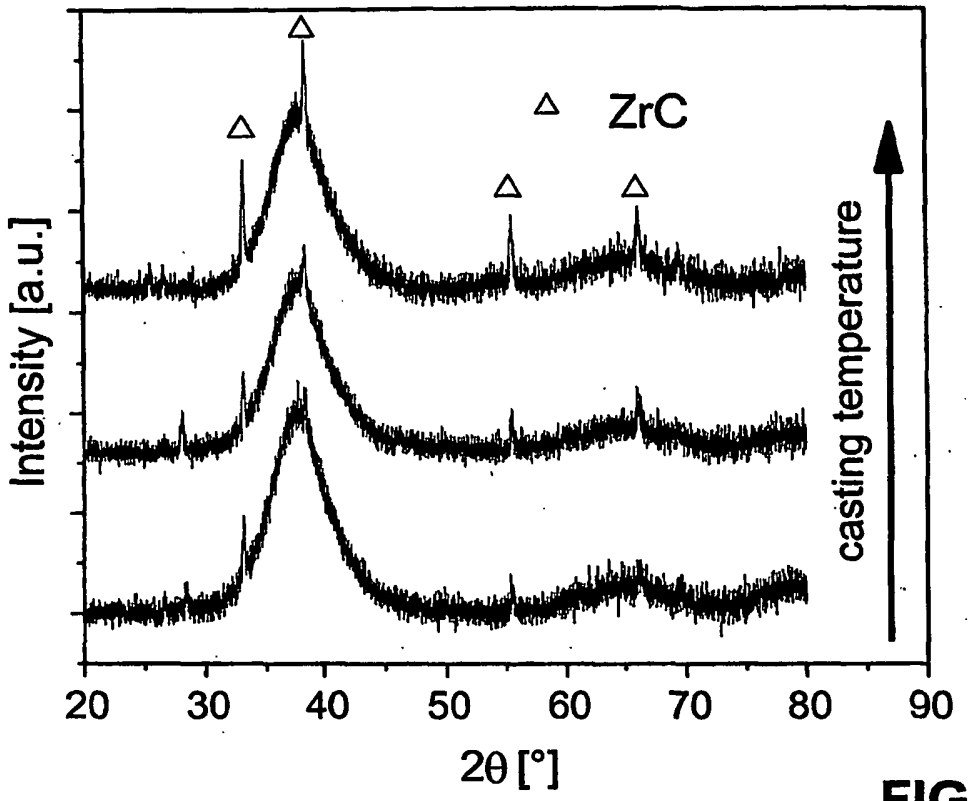

ZrC
Intensity [a.u.]
casting temperature
20
30
40
50
60
70
80
90
2θ [°]

FIG. 3

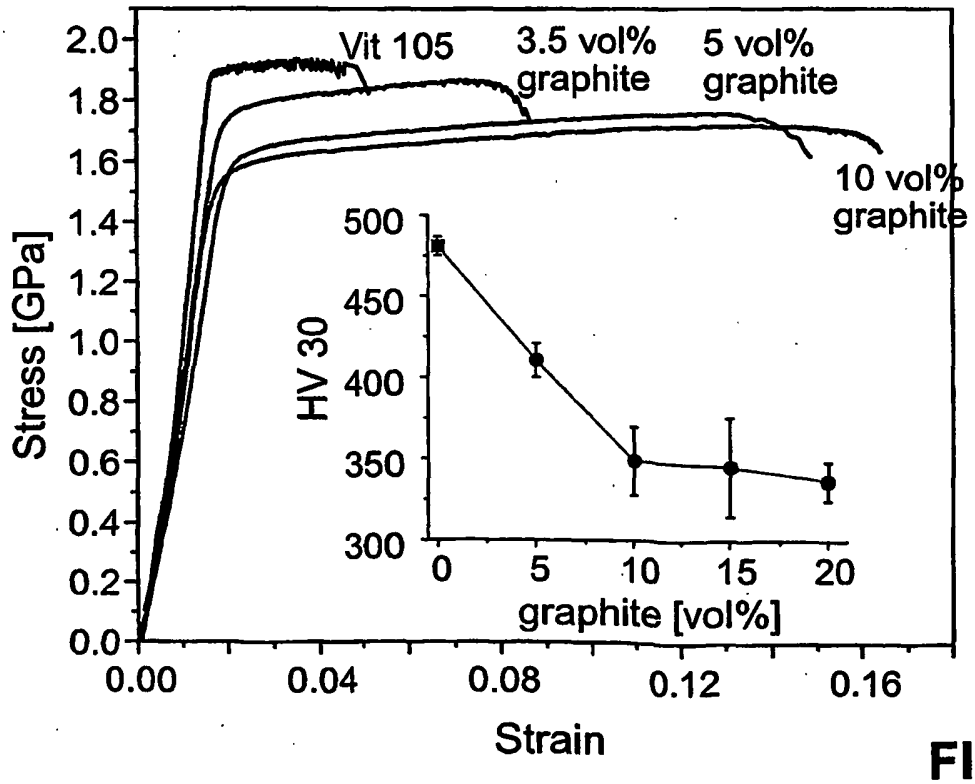

Vit 105
3.5 vol% graphite
5 vol% graphite
10 vol% graphite
Stress [GPa]
Strain
HV 30
graphite [vol%]

FIG. 4

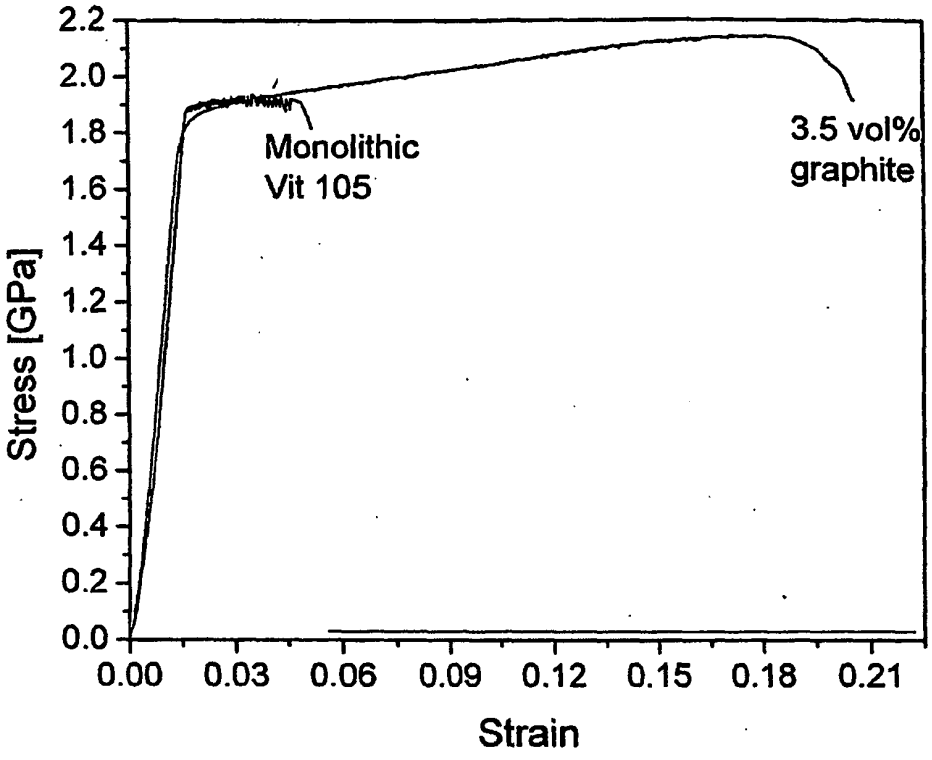

Stress [GPa]
Strain
Monolithic
Vit 105
3.5 vol%
graphite
2.2
2.0
1.8
1.6
1.4
1.2
1.0
0.8
0.6
0.4
0.2
0.0
0.00
0.03
0.06
0.09
0.12
0.15
0.18
0.21

FIG. 5

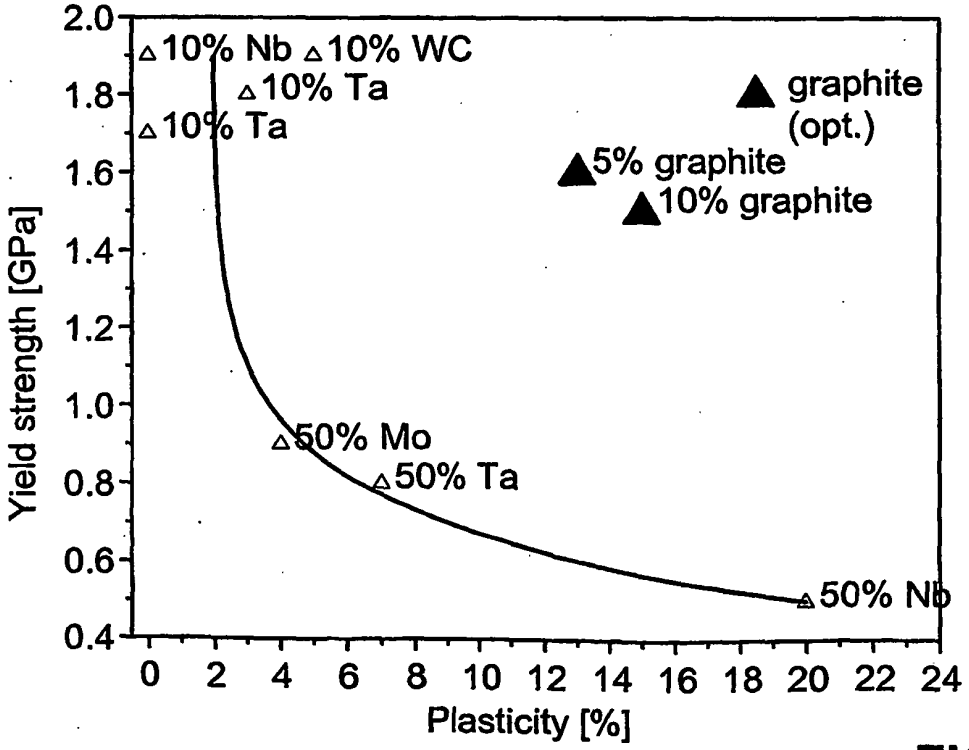

Yield strength [GPa]
Plasticity [%]
10% Nb
10% WC
10% Ta
10% Ta
graphite
(opt.)
5% graphite
10% graphite
50% Mo
50% Ta
50% Nb
2.0
1.8
1.6
1.4
1.2
1.0
0.8
0.6
0.4
0
2
4
6
8
10
12
14
16
18
20
22
24

FIG. 6

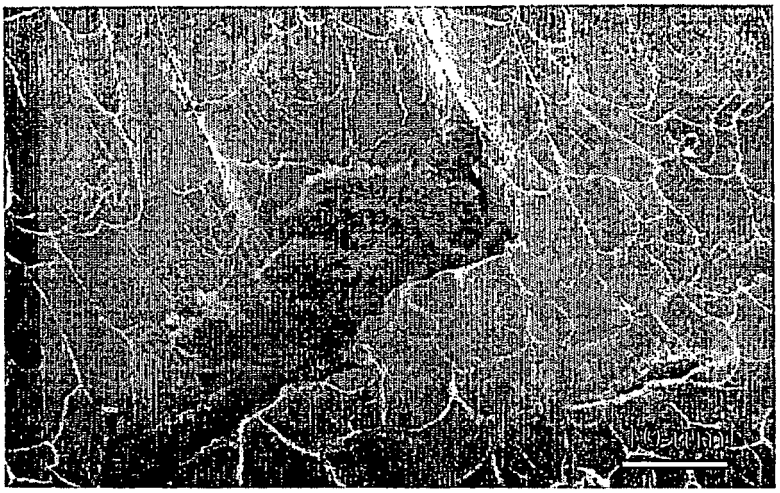


FIG. 7A

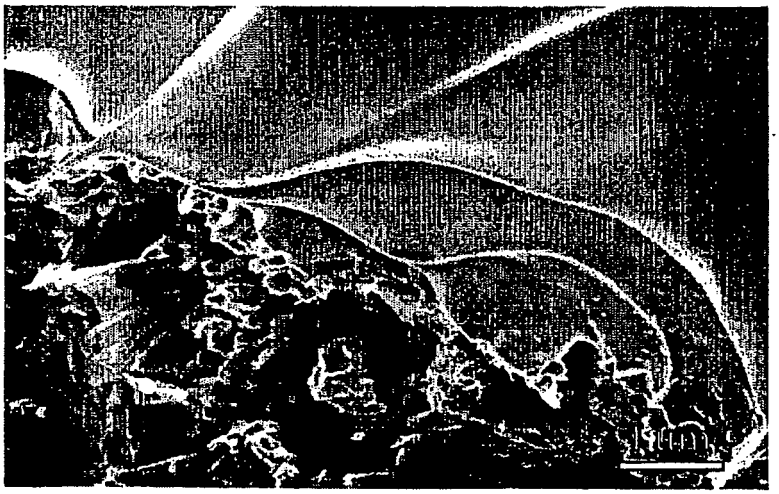


FIG. 7B



FIG. 7C



FIG. 7D



FIG. 7E

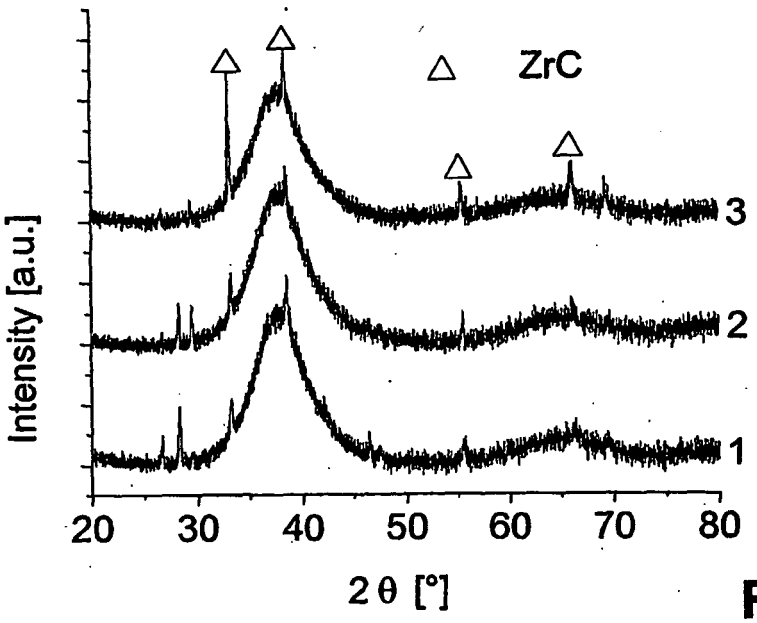

ZrC
Intensity [a.u.]
3
2
1
20
30
40
50
60
70
80
2θ [°]

FIG. 8

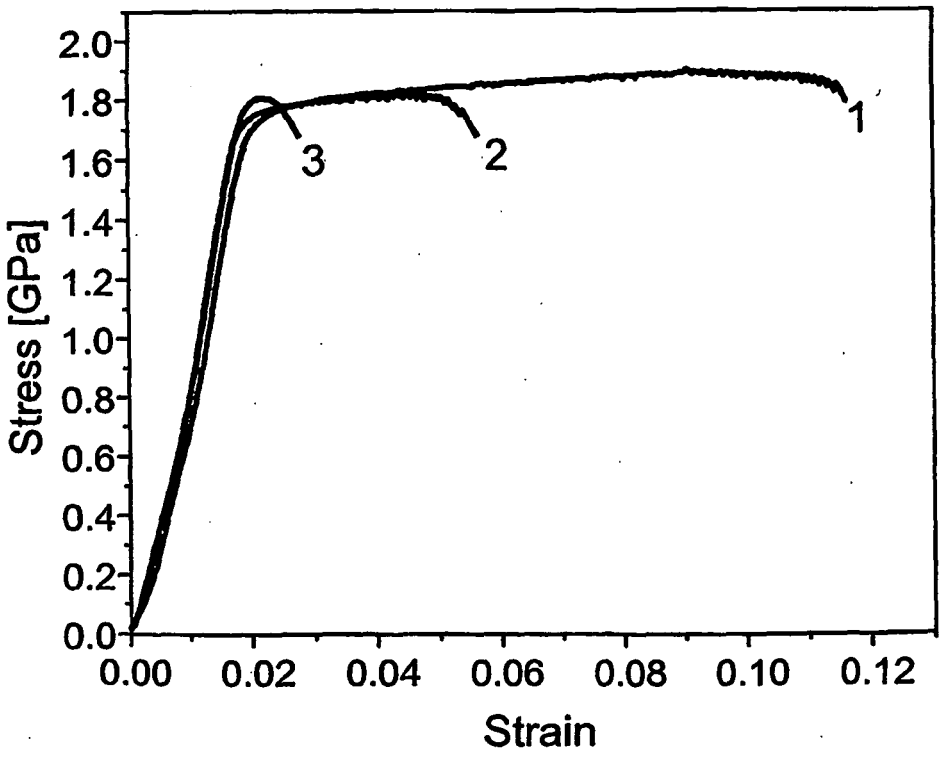

Stress [GPa]
2.0
1.8
1.6
1.4
1.2
1.0
0.8
0.6
0.4
0.2
0.0
0.00
0.02
0.04
0.06
0.08
0.10
0.12
Strain
1
2
3

FIG. 9

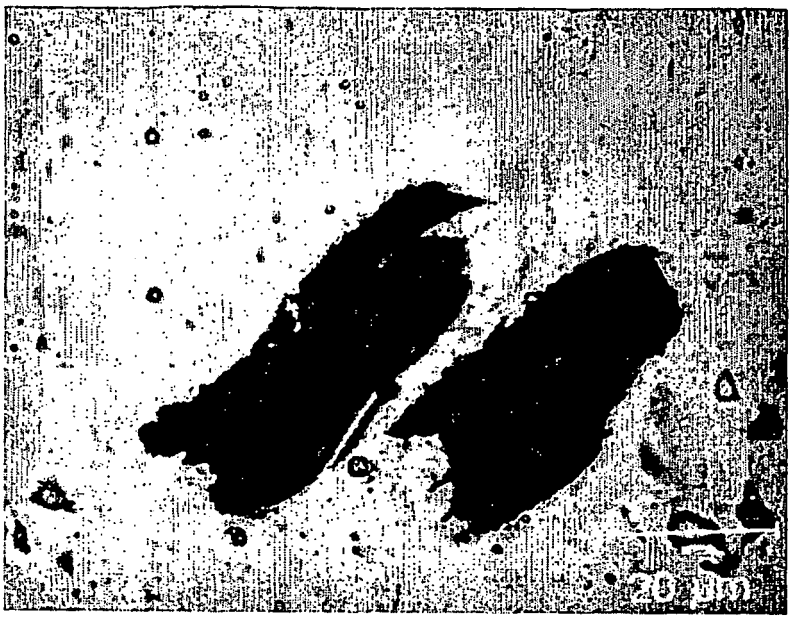


FIG. 10A

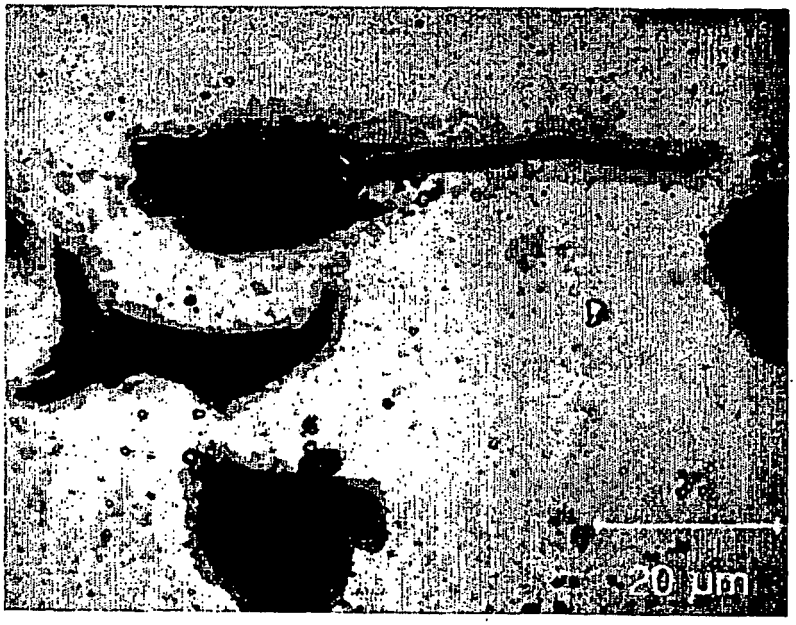


FIG. 10B

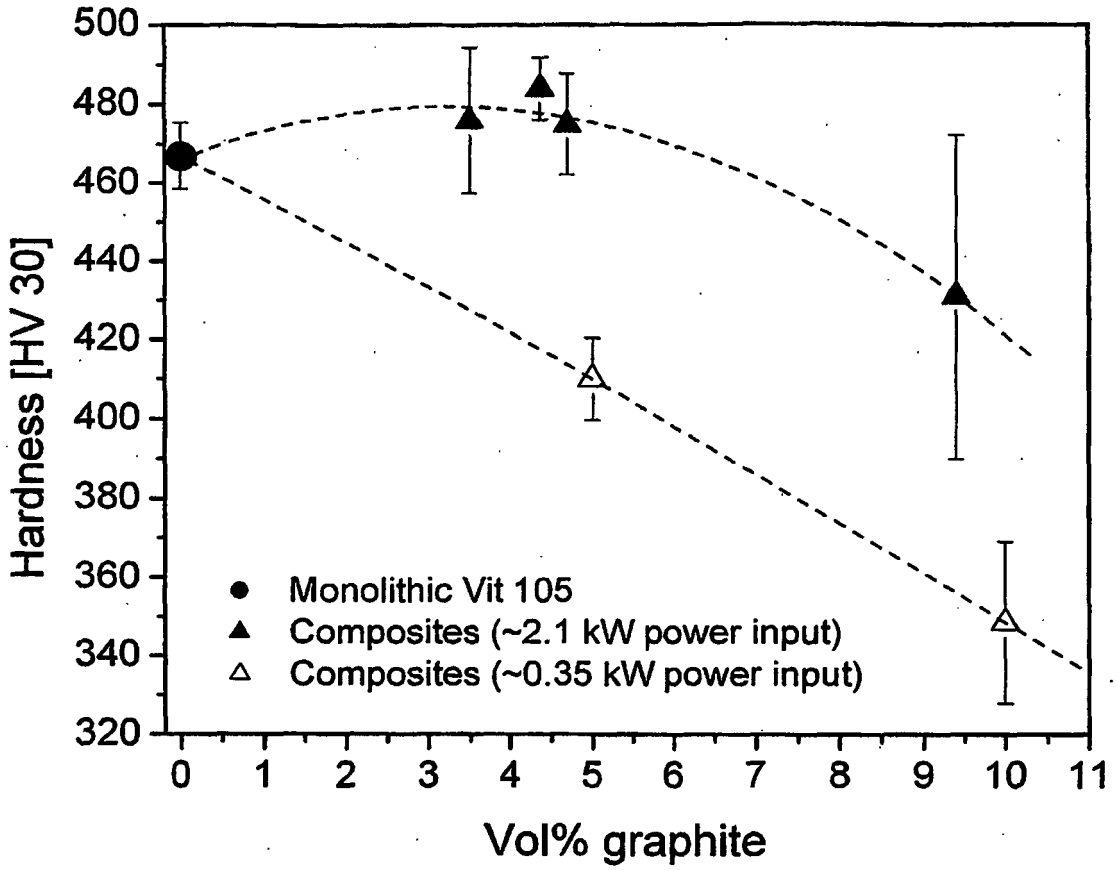

Hardness [HV 30]
500
480
460
440
420
400
380
360
340
320
0
1
2
3
4
5
6
7
8
9
10
11
Vol% graphite
Monolithic Vit 105
Composites (~2.1 kW power input)
Composites (~0.35 kW power input)

FIG. 11

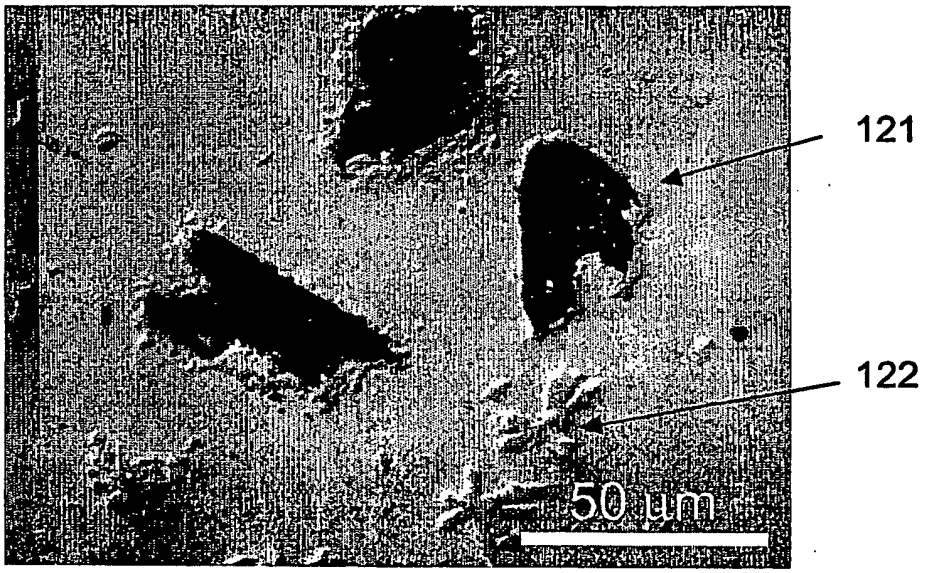

121
122
50 um

FIG. 12

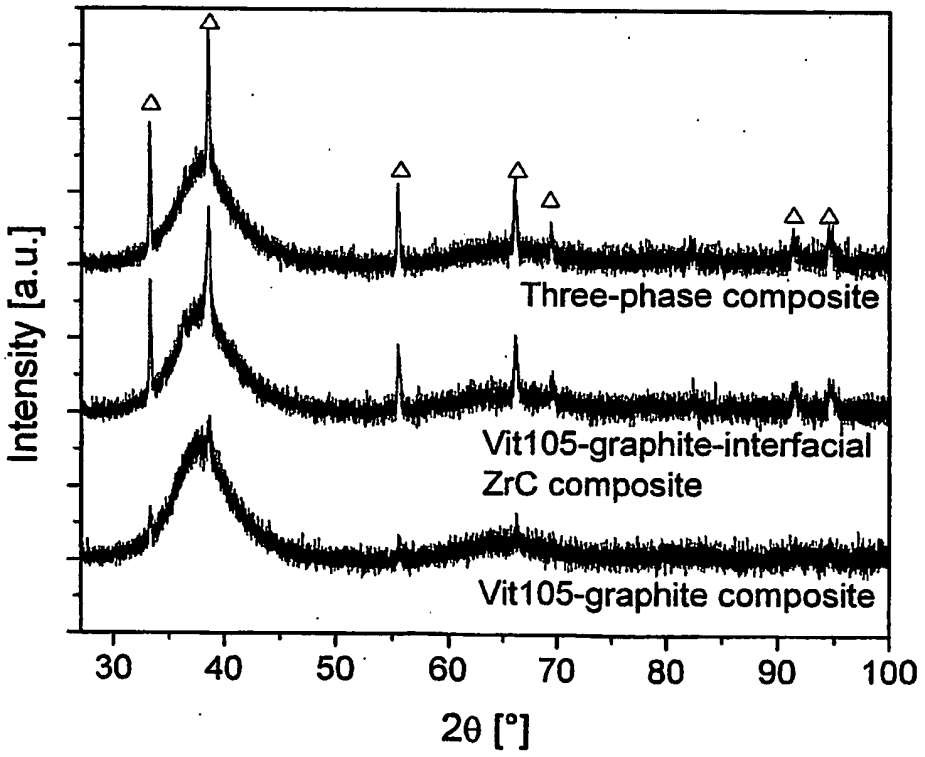

Intensity [a.u.]
Three-phase composite
Vit105-graphite-interfacial ZrC composite
Vit105-graphite composite
30
40
50
60
70
80
90
100
2θ [°]

FIG. 13

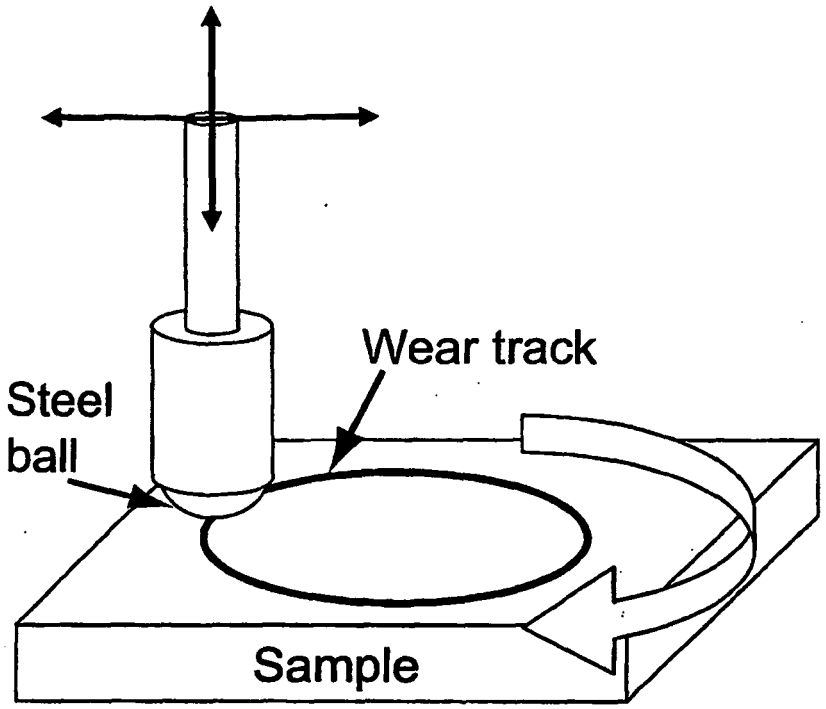

Wear track
Steel ball
Sample

FIG. 14

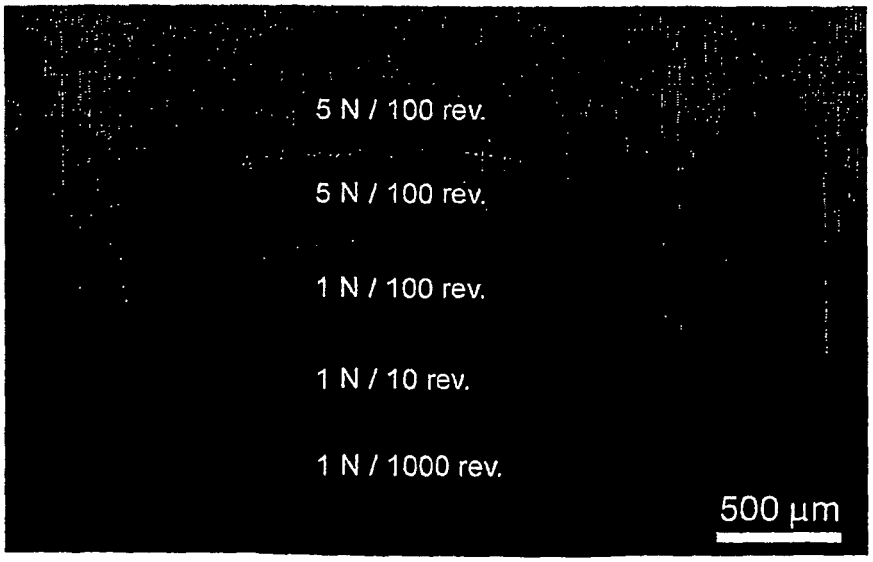

5 N / 100 rev.
5 N / 100 rev.
1 N / 100 rev.
1 N / 10 rev.
1 N / 1000 rev.
500 µm

FIG. 15

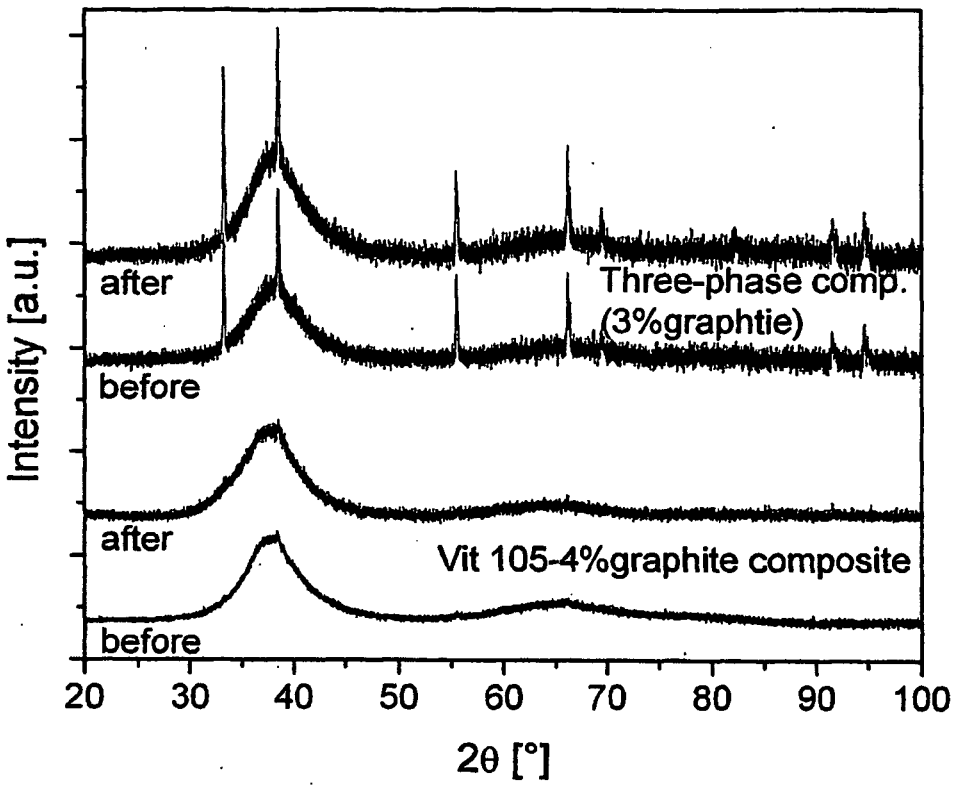

Intensity [a.u.]
after
before
Three-phase comp.
(3%graphtie)
after
before
Vit 105-4%graphite composite
20
30
40
50
60
70
80
90
100
2θ [°]

FIG. 16

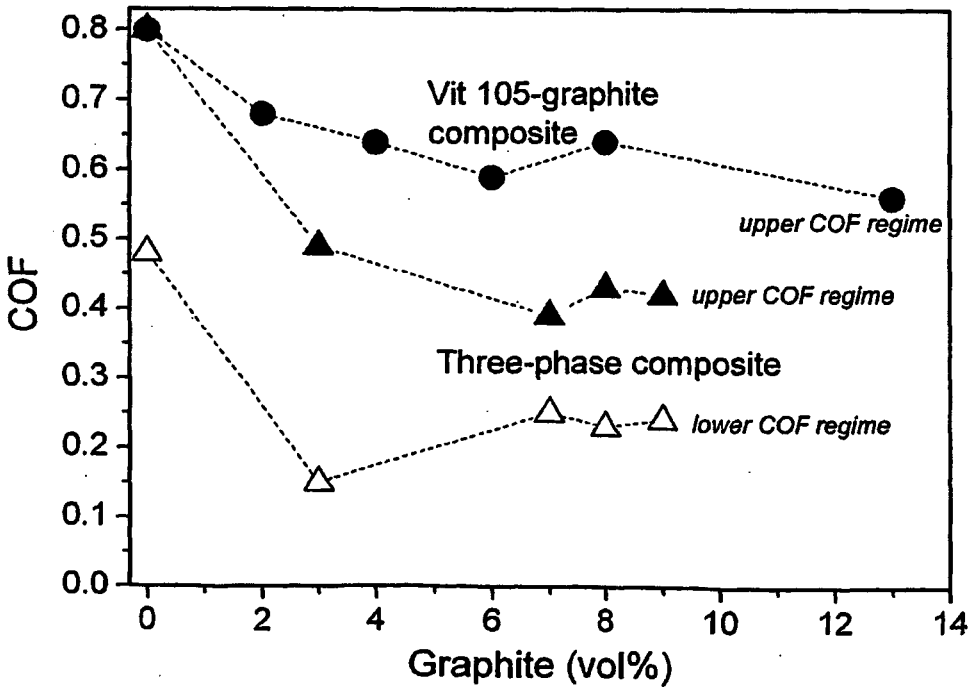

COF
0.0
0.1
0.2
0.3
0.4
0.5
0.6
0.7
0.8
Vit 105-graphite
composite
upper COF regime
upper COF regime
Three-phase composite
lower COF regime
0
2
4
6
8
10
12
14
Graphite (vol%)

FIG. 17

REFERENCES CITED IN THE DESCRIPTION

This list of references cited by the applicant is for the reader's convenience only. It does not form part of the European patent document. Even though great care has been taken in compiling the references, errors or omissions cannot be excluded and the EPO disclaims all liability in this regard.

Patent documents cited in the description

- WO 2006026882 A **[0023]**

Non-patent literature cited in the description

- **Kim, C. P. ; Busch, R. ; Masuhr, A. ; Choi-Yim, H. ; Johnson, W. L.** Processing of Carbon-Fiber-Reinforced Zr41.2Ti13.8Cu12.5Ni10.0Be22.5 Bulk Metallic Glass Composites. *Appl. Phys. Lett.,* 2001, vol. 79, 1456-1458 **[0006]**
- **Bian, Z. et al.** Carbon-nanotube-reinforced Zr52.5Cu17.9Ni14.6Al10Ti5 bulk metallic glass composites. *Appl. Phys. Lett.,* 2002, vol. 81, 4739-4741 **[0006]**
- **Bian, Z. et al.** Carbon-nanotube-reinforced Zr-based bulk metallic glass composites and their properties. *Adv. Funct. Mater.,* 2004, vol. 14, 55-63 **[0006]**
- **Wang, W. H. ; Bai, H. Y.** Carbon-addition-induced bulk ZrTiCuNiBe amorphous matrix composite containing ZrC particles. *Mater. Lett.,* 2000, vol. 44, 59-63 **[0008]**
- **Kato, H. ; Hirano, T. ; Matsuo, A. ; Kawamura, Y. ; Inoue, A.** High strength and good ductility of Zr55Al10Ni5Cu30 bulk glass containing ZrC particles. *Scr. Mater.,* 2000, vol. 43, 503-507 **[0008]**
- **Hirano, T. ; Kato, H. ; Matsuo, A. ; Akihisa ; Inoue, A.** Synthesis and mechanical properties of Zr55Al10Ni5Cu30 bulk glass composites containing ZrC particles formed by the in-situ reaction. *Mater. Trans. JIM,* 2000, vol. 41, 1454-1459 **[0008]**
- **Chen, F. et al.** Crystallization of Zr55Al10Ni5Cu30 Bulk Metallic Glass Composites Containing ZrC Particles. *Mater. Trans. JIM,* 2002, vol. 43, 1-4 **[0008]**
- **Szuecs et al.** Preparation, microstructure and mechanical properties of carbon fiber containing bulk metallic glass composites. *Materials Science Forum,* 2001, vol. 360 (362), 43-48 **[0008]**